Supporting Information

Helicity Control of a Polyaromatic Coordination Capsule through Stereoselective CH-π Interactions

Natsuki Kishida, Hayate Sasafuchi, Tomohisa Sawada, and Michito Yoshizawa*

Laboratory for Chemistry and Life Science, Institute of Innovative Research, Tokyo Institute of Technology, 4259 Nagatsuta, Midori-ku, Yokohama 226-8503, Japan

Contents

- Materials and methods, and references
- Synthesis of compound $\mathbf{3}_{\mathbf{Cl}}$ (^{1}H & ^{13}C NMR and MS spectra)
- Synthesis of compound $\mathbf{3}_{\mathbf{I}}$ (^{1}H & ^{13}C NMR and MS spectra)
- Synthesis of ligand **2** (^{1}H & ^{13}C NMR, COSY, HSQC, and MS spectra)
- Formation of **1** (^{1}H & ^{13}C NMR, HSQC, and MS spectra)
- Formation of **1•αGlc^{Me}**, **1•βGlc^{Me}**, **1•αGal^{Me}**, **1•βGal^{Me}**, **1•αMan^{Me}**, and **1•Fru^{Me}** (^{1}H NMR, HSQC, and/or NOESY spectra)
- Formation of **1”•αGlc^{Me}** (^{1}H NMR and MS spectra)
- Competitive binding experiments
- UV-visible and CD spectra of **1•αGal^{Me}**, **1•βGal^{Me}**, **1•αMan^{Me}**, and **1•Fru^{Me}**
- Theoretical studies of (*P*)/(*M*)-**1** and (*P*)/(*M*)-**1•αGlc^{Me}**
- EXSY NMR spectra of **1•βGal^{Me}**

Materials and methods

NMR: Bruker AVANCE-HD500 (500 MHz), MALDI-TOF MS: Bruker ultrafleXtreme, ESI-TOF MS: Bruker micrOTOF II, UV-visible: JASCO V-670DS, FT-IR: SHIMADZU IRSpirit-T, CD: JASCO J-820.

Solvents and reagents: TCI Co., Ltd., FUJIFILM Wako Chemical Co., Kanto Chemical Co., Inc., Sigma-Aldrich Co., and Cambridge Isotope Laboratories, Inc. Compounds: Compound $\mathbf{3}_{\mathbf{MOE}}$, capsule **1"**, pentamethylated α/β-D-glucose mixture (1:4) and fructose were synthesized according to ref. S1, S2, and S3, respectively.

Calculations

DFT calculation: Gaussian 16 program (Rev. C.01) package, Molecular mechanics calculation: Forcite module, BIOVIA Materials Studio 2020, version 20.1.0.5 (Dassault Systèmes Co.), NCI analysis: NCIPLOT 4.0, Calculations: DFT and TD-DFT calculations of capsule **1** (R = H) and its host-guest complexes were performed for the geometry optimizations (CAM-B3LYP/LanL2DZ (Pd), 6-31G(d,p) (others) level of theory).

References

[S1] N. Kishida, K. Matsumoto, Y. Tanaka, M. Akita, H. Sakurai, M. Yoshizawa, *J. Am. Chem. Soc.* **2020**, *142*, 9599–9603.

[S2] N. Kishida, Y. Tanaka, M. Yoshizawa, *Chem. Eur. J.* **2022**, *28*, e202202075.

[S3] Z. R. Laughrey, S. E. Kiehna, A. J. Riemen, M. L. Waters, *J. Am. Chem. Soc.* **2008**, *130*, 14625–14633.

[S4] C. L. D. Gibb, B. C. Gibb, *J. Am. Chem. Soc.* **2004**, *126*, 11408–11409.

[S5] M. Yamashina, S. Matsuno, Y. Sei, M. Akita, M. Yoshizawa, *Chem. Eur. J.* **2016**, *22*, 14147–14150.

Synthesis of compound 3_{Cl} NKS1085, 1120

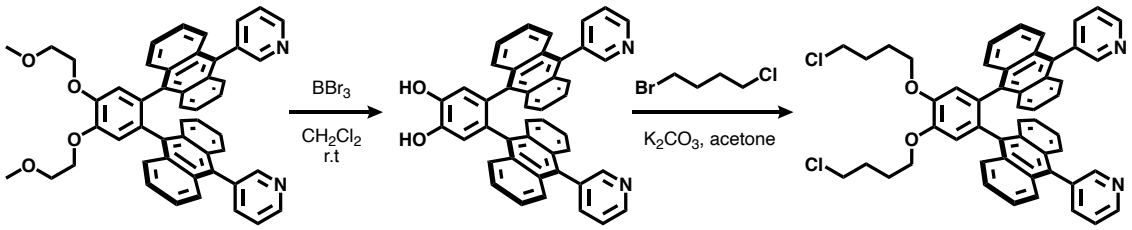

Compound $\mathbf{3_{MOE}}$ (0.113 g, 0.154 mmol) was added to a 100 mL glass flask filled with N_2. Dry CH_2Cl_2 (40 mL) was added to the flask. A 1 M CH_2Cl_2 solution of BBr_3 (2.1 mL, 2.1 mmol) was added to the flask at 0 ºC, and then the mixture was stirred at r.t. for 3 h. After addition of H_2O (30 mL), the mixture was neutralized by adding 1N NaOH aq. The product was extracted with CH_2Cl_2, and then the obtained organic layer was dried over $MgSO_4$, filtrated, and concentrated under reduced pressure to afford crude $\mathbf{3_{OH}}$ (94.8 mg, 0.154 mmol, 100%) as a brown solid.

Compound $\mathbf{3_{OH}}$ (94.8 mg, 0.154 mmol) and K_2CO_3 (0.503 g, 3.64 mmol) were added to a 100 mL glass flask filled with N_2. Dry acetone (20 mL) was added to the flask, and then the mixture was stirred at 70 ºC for 30 min. After an acetone solution (15 mL) of 1-bromo-4-chlorobutane (0.252 g, 1.47 mmol) was added to the flask, the mixture was stirred at 70 ºC overnight. The mixture was concentrated under reduced pressure. The product was extracted with CH_2Cl_2 and the obtained organic layer was dried over Na_2SO_4, filtrated, and concentrated under reduced pressure. The obtained crude product was purified by GPC ($CHCl_3$) to afford ligand $\mathbf{3_{Cl}}$ (73.4 mg, 92.0 μmol, 60%) as a yellow solid.

$\mathbf{3_{OH}}$: ^{1}H NMR (400 MHz, CD_3OD, after the addition of conc. HCl aq. (one drop), r.t.): δ 8.94-8.89 (m, 2H), 8.75 (s, 1H), 8.33-8.30 (m, 2H), 8.15-8.07 (m, 7H), 7.24-7.12 (m, 14H).

$\mathbf{3_{Cl}}$: ^{1}H NMR (400 MHz, $CDCl_3$, r.t.): δ 8.68 (m, 2H), 8.49-8.48 (m, 1H), 8.04 (br, 1H), 7.99-7.89 (m, 4H), 7.58 (dd, J = 7.9 Hz, 1H), 7.44-7.39 (m, 4H), 7.21-7.14 (m, 5H), 7.06-7.02 (m, 4H), 6.99-6.92 (m, 4H), 4.24 (br, 4H), 3.76 (br, 4H), 2.13 (br, 4H). ^{13}C NMR (100 MHz, $CDCl_3$, r.t.): δ 151.4 (CH), 148.6 (CH), 148.2 (C_q), 138.6 (CH), 136.4 (C_q), 134.8 (C_q), 132.5 (C_q), 131.7 (C_q), 129.6 (C_q), 129.4 (C_q), 127.8-127.6 (CH), 125.5 (CH), 124.9 (CH), 124.0 (CH), 123.1 (CH), 118.0 (CH), 68.6 (CH_2), 44.9 (CH_2), 29.7 (CH_2), 26.8 (CH_2). FT-IR (ATR, cm^{-1}): 2961, 1487, 1440, 1393, 1262, 1240, 1225, 1157, 1091, 1053, 1027, 911, 807, 767, 717, 687, 613, 419. HR MS (ESI, CH_3OH): m/z Calcd. for $C_{52}H_{43}Cl_2N_2O_2$ 797.2696 $[M + H]^+$, Found 797.2695.

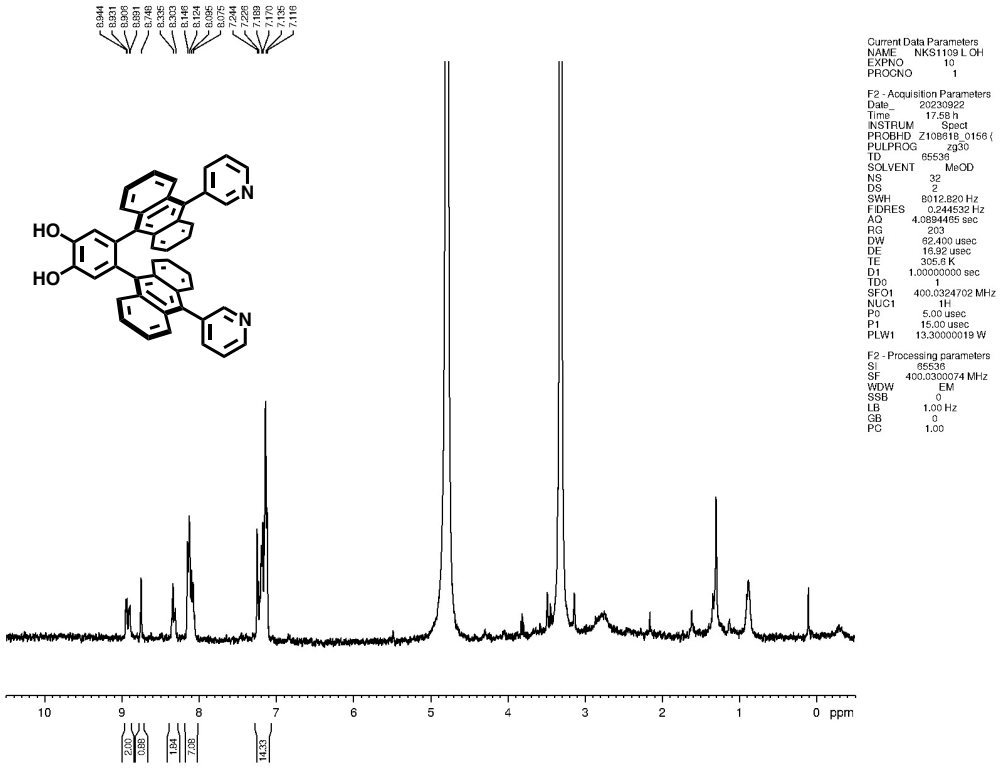

Figure S1. ^{1}H NMR spectrum (500 MHz, CD_3OD, r.t., after the addition of conc. HCl aq. (one drop)) of $\mathbf{3_{OH}}$.

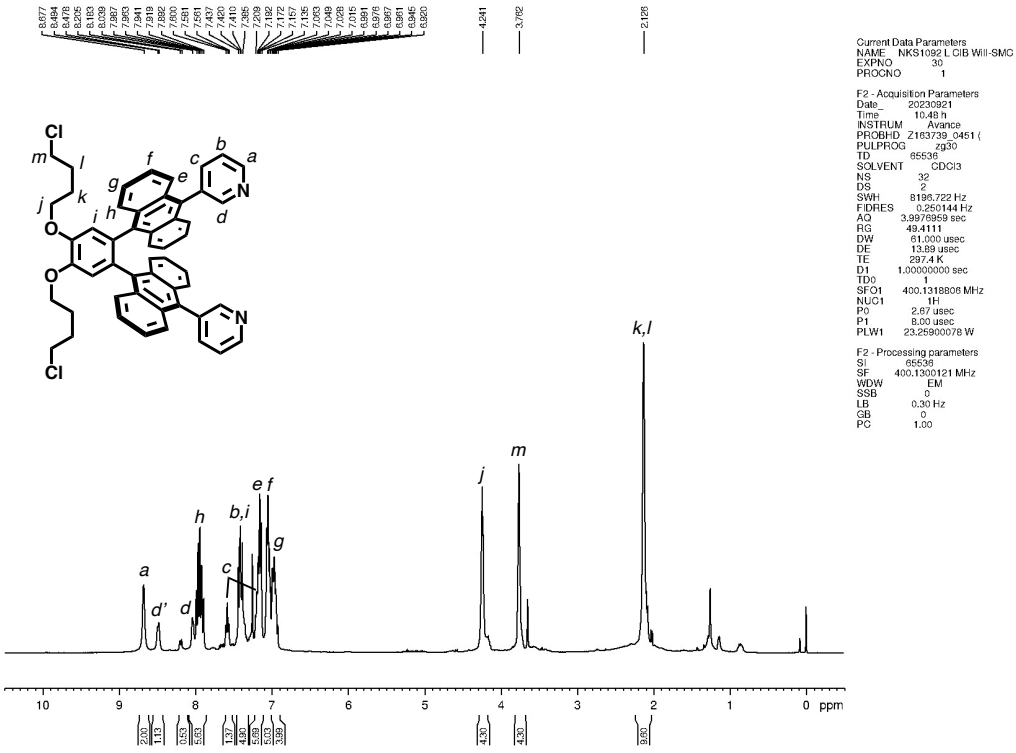

Figure S2. ^{1}H NMR spectrum (400 MHz, $CDCl_3$, r.t.) of $\mathbf{3_{Cl}}$.

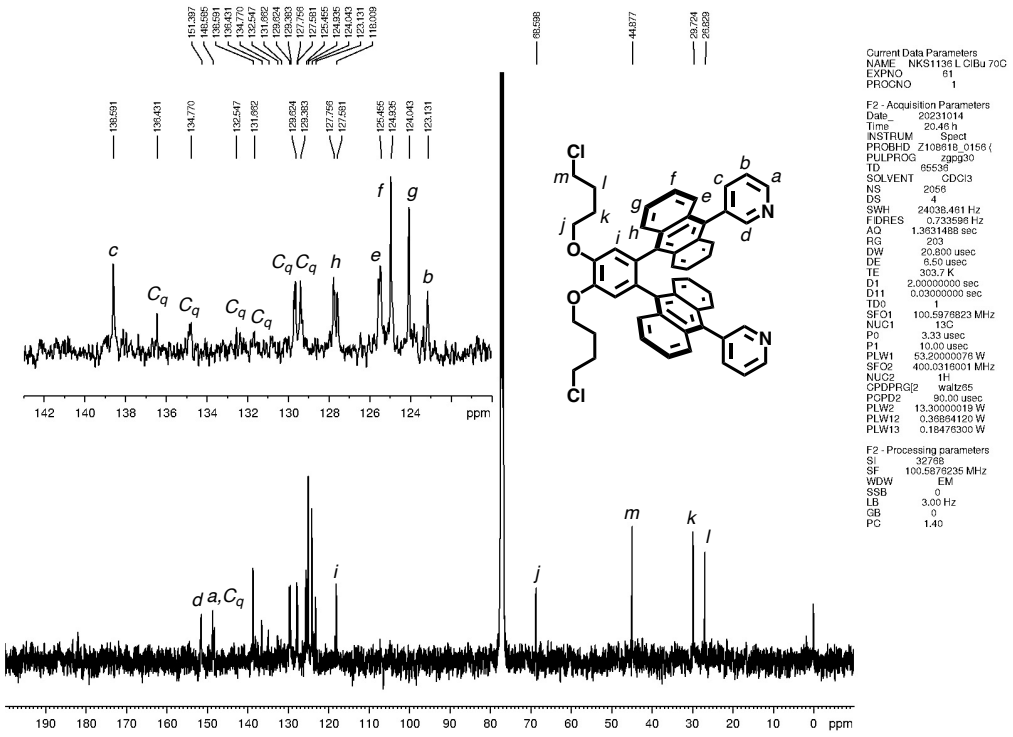

Figure S3. ^{13}C NMR spectrum (100 MHz, $CDCl_3$, r.t.) of $\mathbf{3_{Cl}}$.

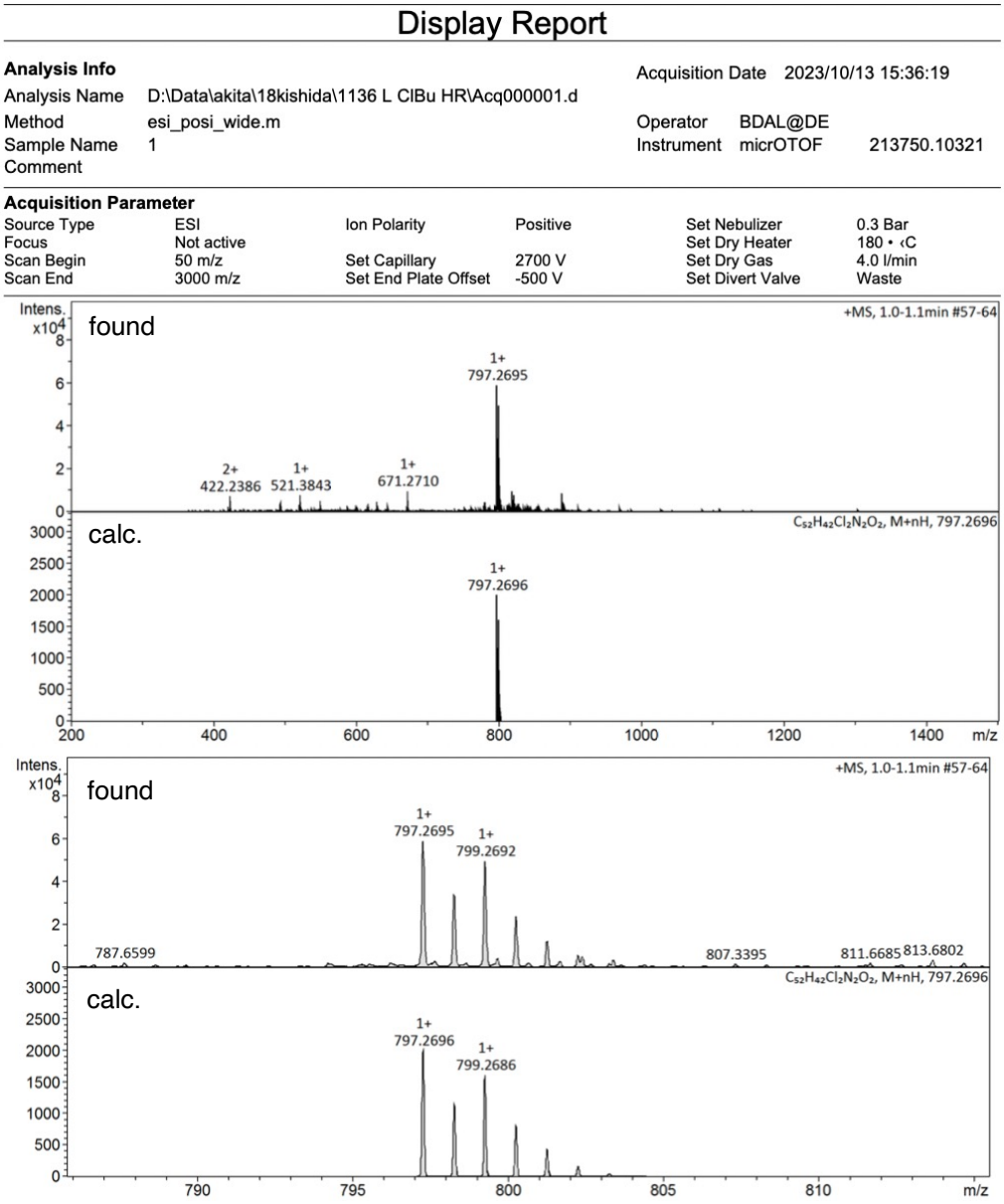

Figure S4. HR MS spectrum (ESI, CH_3OH) of $\mathbf{3}_{Cl}$.

Synthesis of compound 3_I NKS1151

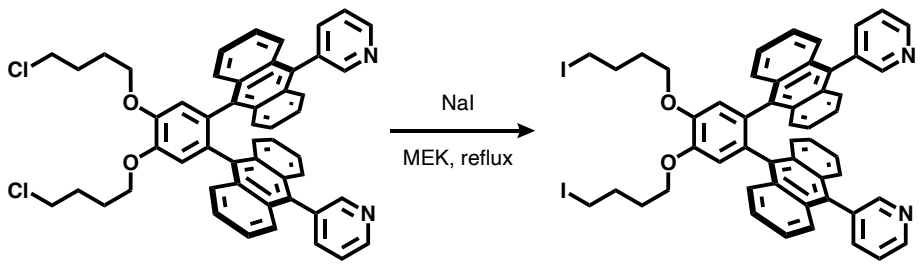

Compound $\mathbf{3}_{Cl}$ (163 mg, 0.205 mmol), sodium iodide (1.23 g, 8.20 mmol), and dry methyl ethyl ketone (MEK; 40 mL) were added to a 200 mL glass flask filled with N_2, and then the mixture was stirred at 85 ºC overnight. The reaction mixture was

concentrated under reduced pressure. After addition of water, the crude product was extracted with CH_2Cl_2. The obtained organic layer was dried over Na_2SO_4, filtrated, and concentrated under reduced pressure. The crude product was purified by GPC ($CHCl_3$) to afford **3$_I$** (99.9 mg, 0.102 mmol, 50%) as a yellow solid.

^{1}H NMR (100 MHz, $CDCl_3$, r.t.): δ 8.68 (br, 2H), 8.50-8.48 (m, 1H), 8.04 (br, 1H), 7.98-7.89 (m, 4H), 7.58 (m, 1H), 7.44-7.37 (m, 4H), 7.18-7.13 (m, 5H), 7.07-7.01 (m, 4H), 6.99-6.92 (m, 4H), 4.24 (t, J = 5.0 Hz, 4H), 3.42 (t, J = 6.8 Hz, 4H), 2.22-2.09 (m, 8H).

^{13}C NMR (125 MHz, $CDCl_3$, r.t.): δ 151.6-151.5 (CH), 148.7-148.6 (CH), 148.2-148.1 (C_q), 138.6-138.4 (CH), 136.4-136.2 (C_q), 134.8-134.7 (C_q), 132.6-132.3 (C_q), 131.9-131.7 (C_q), 129.7-129.6 (C_q), 129.4 (C_q), 127.8-127.6 (CH), 125.6-125.4 (CH),125.0 (CH), 124.1 (CH), 123.3-123.0 (CH), 118.0 (CH), 68.3 (CH_2), 30.7 (CH_2), 30.3 (CH_2), 6.7 (CH_2). FT-IR (ATR, cm^{-1}): 2924, 1514, 1440, 1386, 1243, 1198, 1156, 1091 ,1027, 928, 809, 769, 718, 687, 614, 419. HR MS (ESI, CH_3OH): m/z Calcd. for $C_{52}H_{43}I_2N_2O_2$ 981.1409 [M + H]$^+$, Found 981.1413.

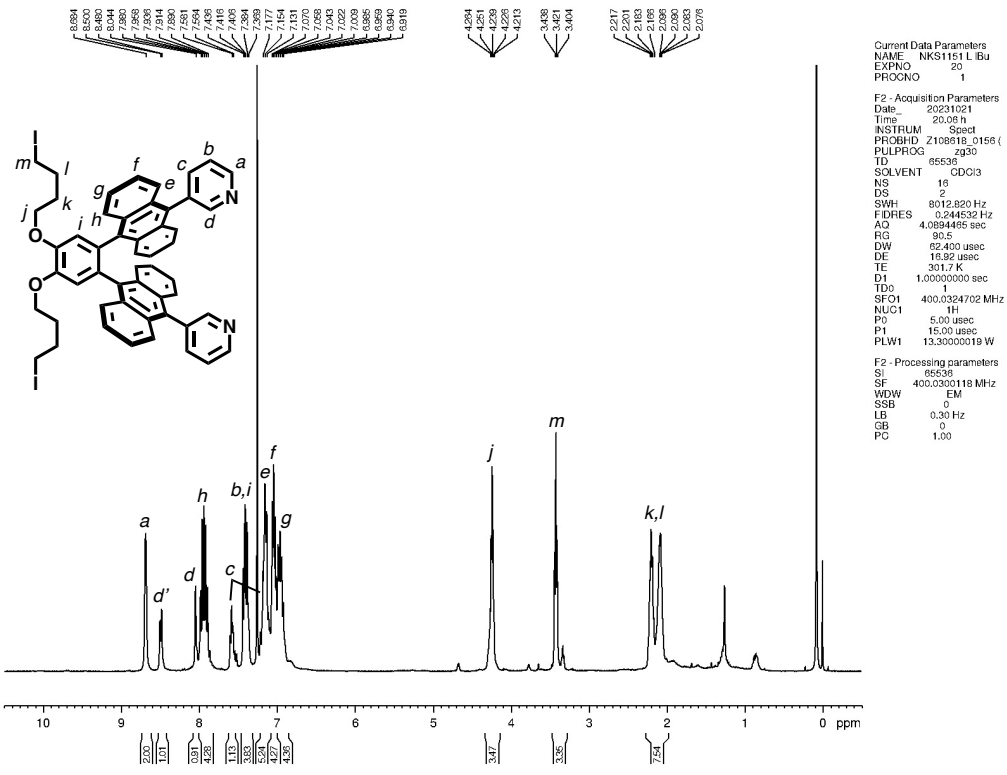

Figure S5. ^{1}H NMR spectrum (400 MHz, $CDCl_3$, r.t.) of **3$_I$**.

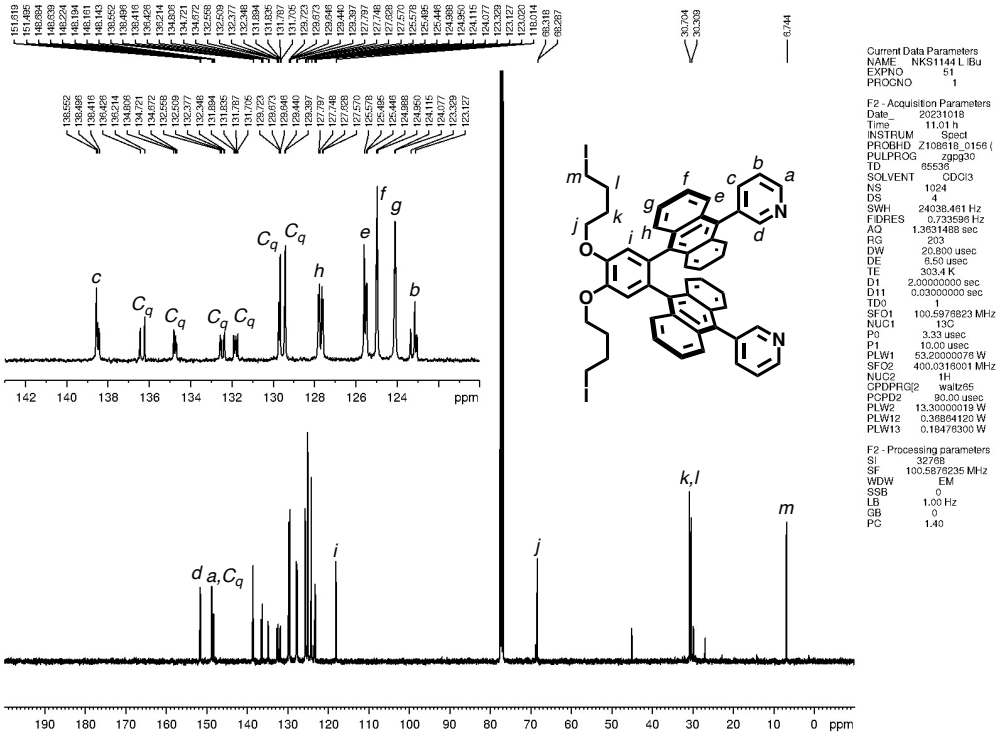

Figure S6. ^{13}C NMR spectrum (100 MHz, $CDCl_3$, r.t.) of $\mathbf{3_I}$.

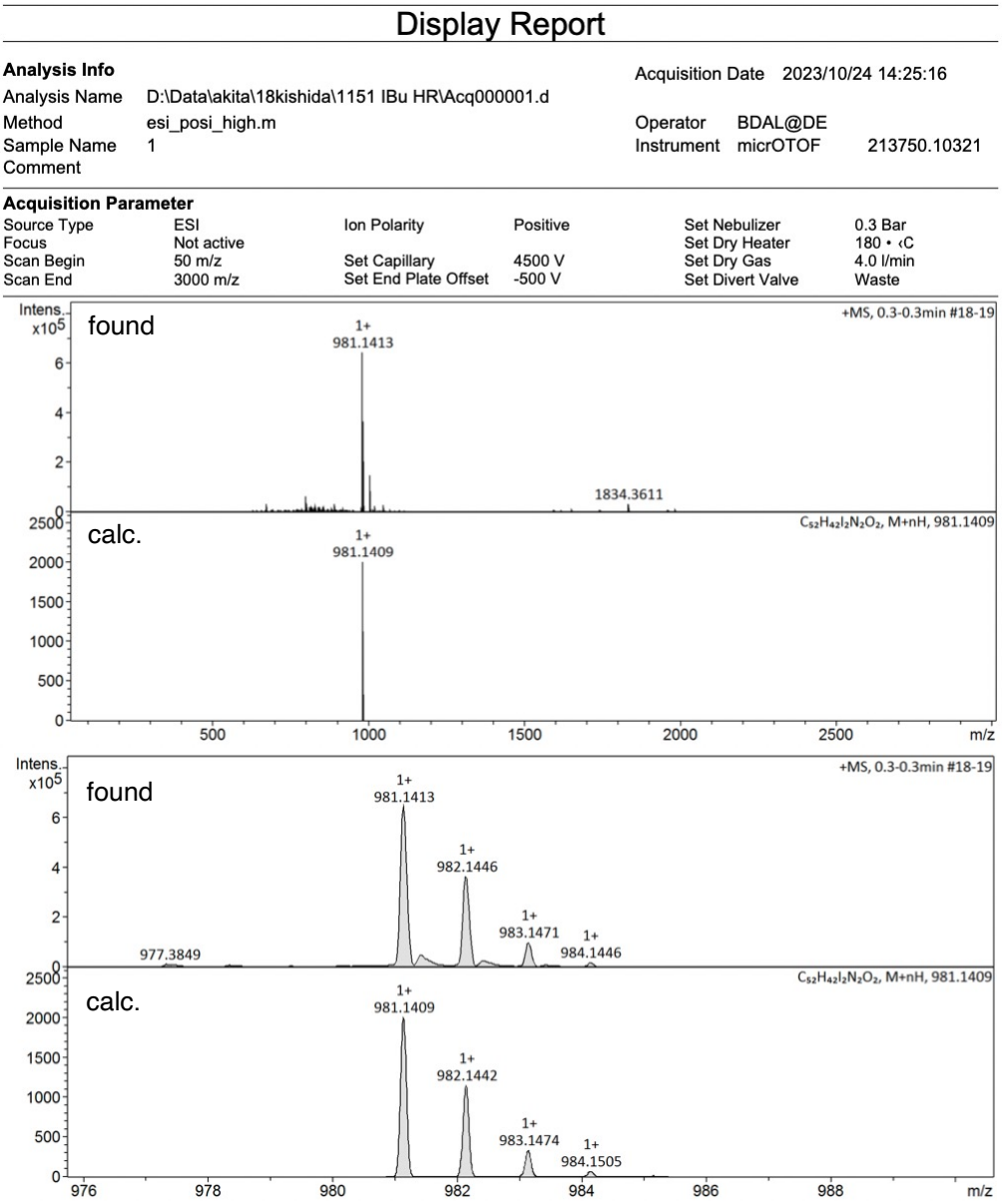

Figure S7. HR MS spectrum (ESI, CH_3OH) of $\mathbf{3_I}$.

Synthesis of ligand 2

NKS1149, 1150

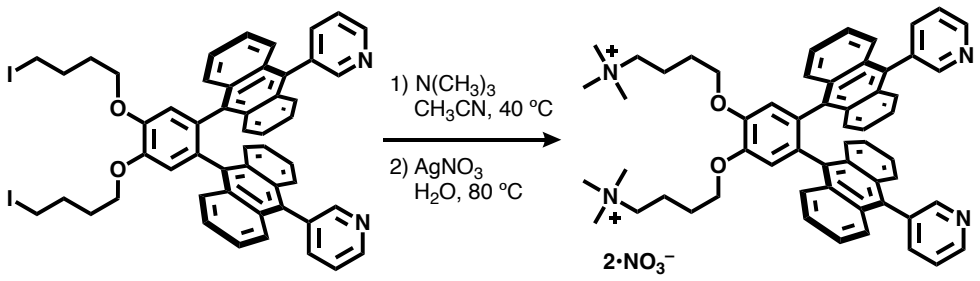

Compound $\mathbf{3_I}$ (33.3 mg, 34.0 μmol) and an CH_3CN solution (2 M) of trimethylamine (10 mL, 20 mmol) were added to a sealed 50 mL flask. The mixture was

stirred at 40 ºC overnight. The resultant mixture was concentrated under reduced pressure to afford crude **4** as a yellow solid. The crude **4** (ca. 37 mg, 34 μmol), $AgNO_3$ (1.73 mg, 102 μmol), and H_2O (5 mL) were added to a test tube, and then the mixture was stirred at 80 ºC overnight. The resultant mixture was concentrated under reduced pressure. After addition of CH_3OH, the resultant solution was filtered through a membrane filter and then concentrated under reduced pressure. The crude product was washed with hexane to afford ligand **2** (30.1 mg, 31.1 μmol; 91% in 2 steps) as a yellowish-orange solid.

Compound **4**: ^{1}H NMR (500 MHz, CD_3OD, r.t.): δ 8.67 (m, 2H), 8.32-8.31 (m, 1H), 7.98 (d, J = 8.8 Hz, 1H), 7.94-7.84 (m, 4H), 7.73-7.70 (m, 1H), 7.63-7.51 (m, 4H), 7.40-7.30 (m, 1H), 7.13-6.95 (m, 12H), 4.39-4.33 (m, 4H), 3.63-3.51 (m, 4H), 3.19 (s, 18H), 2.10-2.06 (m, 8H). ESI-TOF MS (CH_3OH): m/z 422.32 $[M - 2\bullet I^-]^{2+}$, 971.58 $[M - I^-]^+$.

Ligand **2**: ^{1}H NMR (400 MHz, CD_3OD, r.t.): δ 8.64 (br, 2H), 8.35 (br, 1H), 7.99-7.89 (m, 5H), 7.72 (d, J = 7.6 Hz, 1H), 7.61 (m, 1H), 7.53-7.47 (m, 3H), 7.30-7.24 (m, 1H), 7.10-6.93 (m, 12H), 4.33 (t, J = 6.0 Hz, 4H), 3.55 (m, 4H), 3.21 (s, 18H), 2.12 (m, 4H), 2.05 (m, 4H). ^{13}C NMR (100 MHz, $CDCl_3$, r.t.): δ 151.7 (CH), 149.8 (C_q), 149.2 (CH), 140.7 (CH), 137.8 (C_q) , 136.7 (C_q), 134.1 (C_q), 132.5 (C_q), 131.0 (C_q), 130.7 (C_q), 129.0-128.8 (CH), 126.3(C H), 126.2 (CH), 125.3 (CH), 125.3 (CH), 119.8 (CH), 70.0 (CH_2), 67.6 (CH_2), 53.6 (CH_3), 27.4 (CH_2), 21.1 (CH_2). FT-IR (ATR, cm^{-1}): 3034, 2926, 1483, 1440, 1319, 1242, 1201, 1157, 1088, 1028, 913, 830, 770, 720, 688, 649, 614. ESI-TOF MS (CH_3OH): m/z 422.26 $[M - 2\bullet NO_3^-]^{2+}$, 906.49 $[M - NO_3^-]^+$.

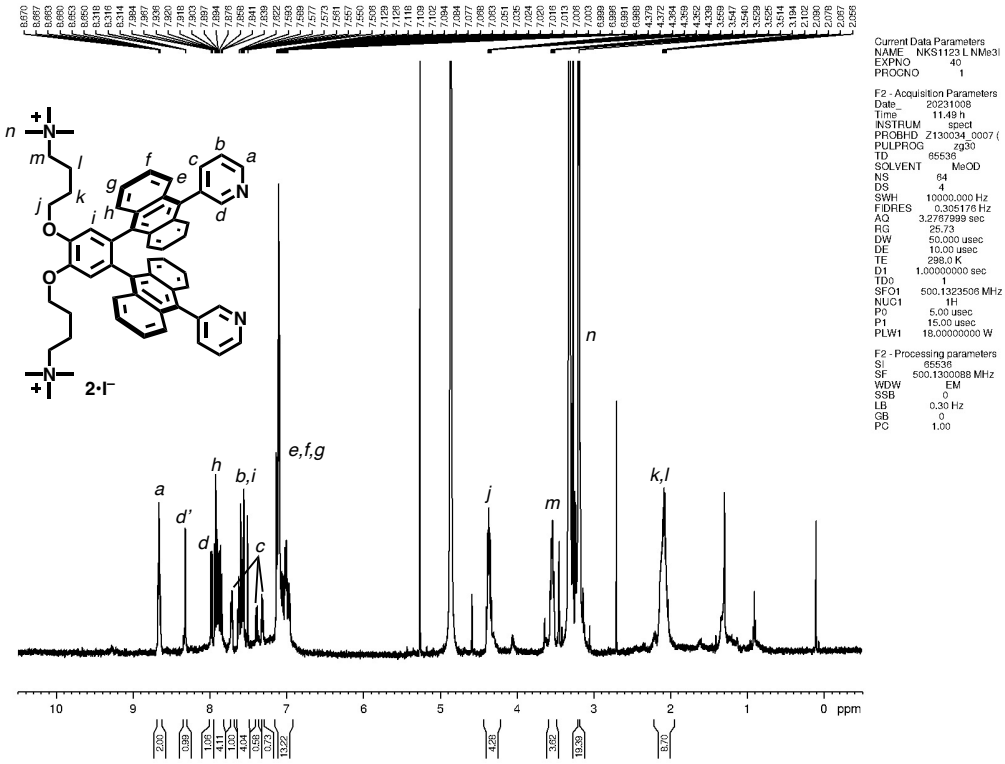

Figure S8. ^{1}H NMR spectrum (500 MHz, CD_3OD, r.t.) of **4**.

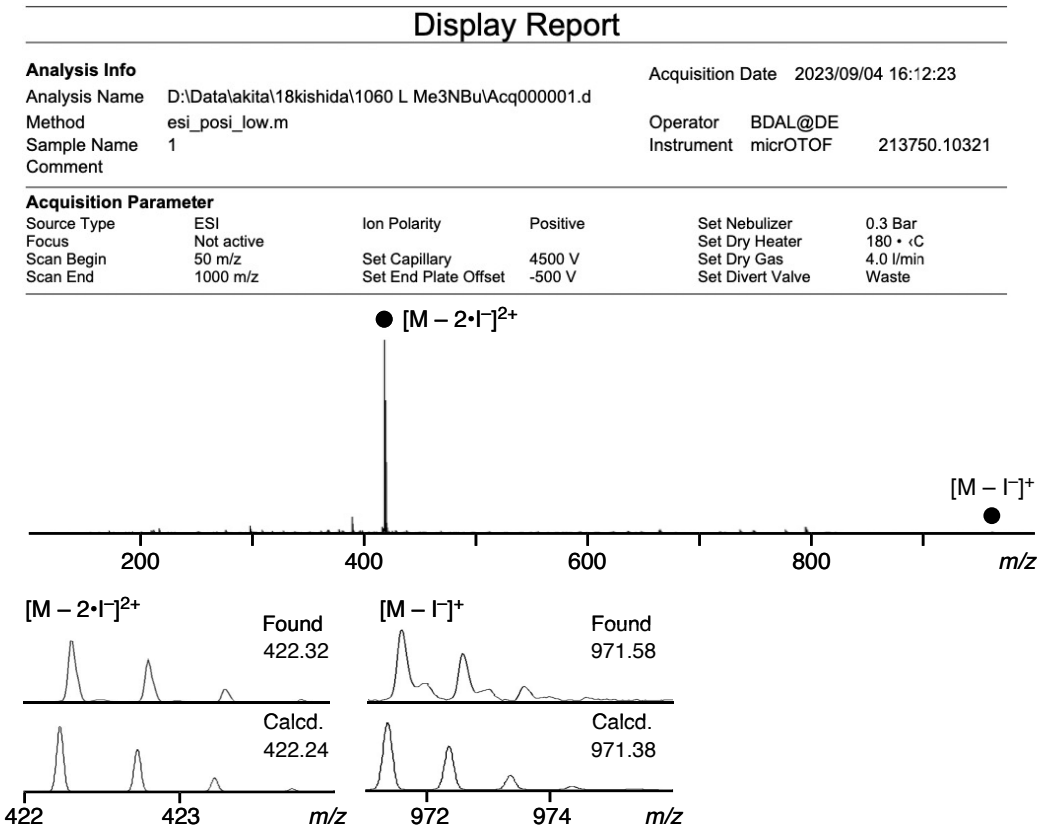

Figure S9. ESI-TOF MS spectrum (CH_3OH) of **4**.

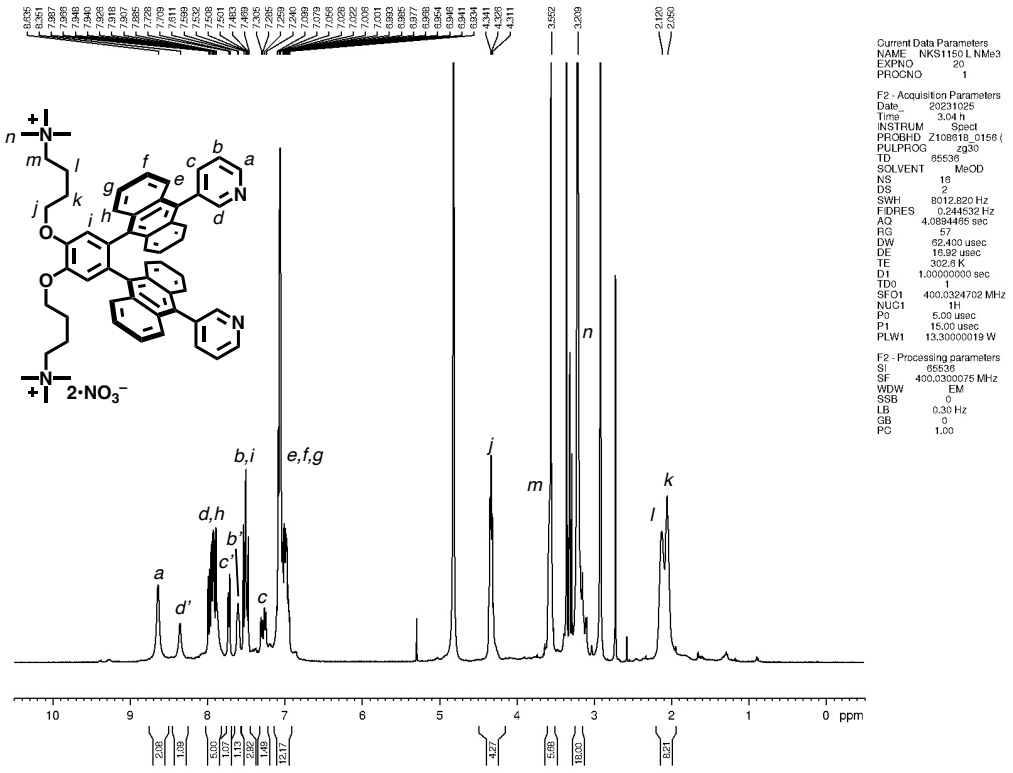

Figure S10. ^{1}H NMR spectrum (400 MHz, CD_3OD, r.t.) of **2**.

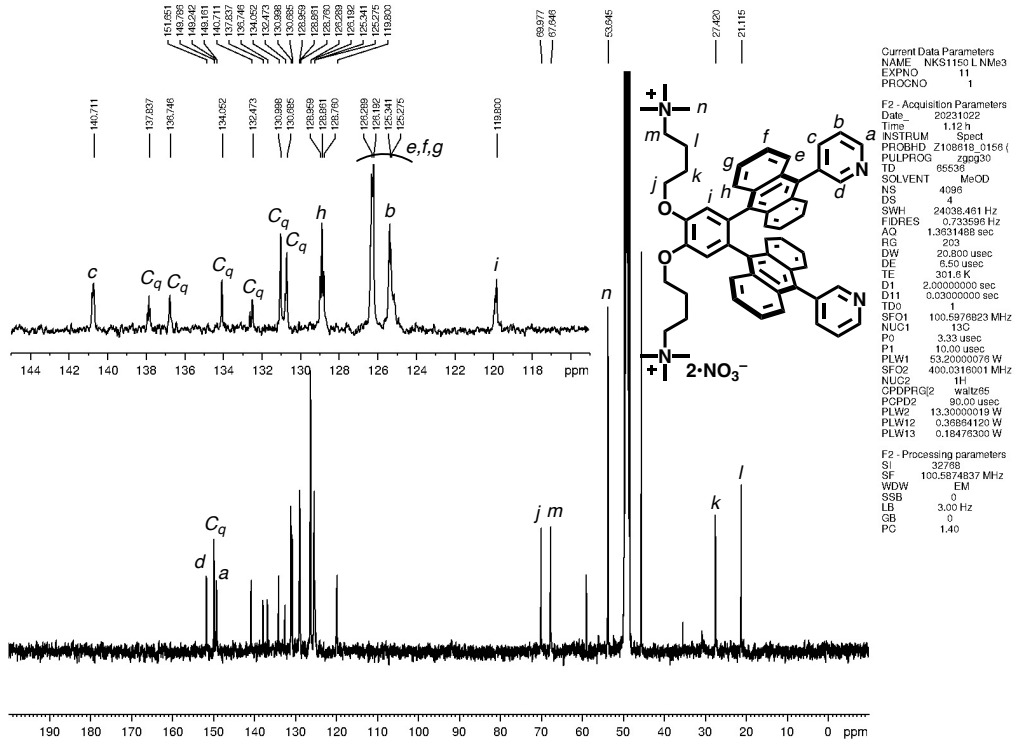

Figure S11. ^{13}C NMR spectrum (100 MHz, CD_3OD, r.t.) of **2**.

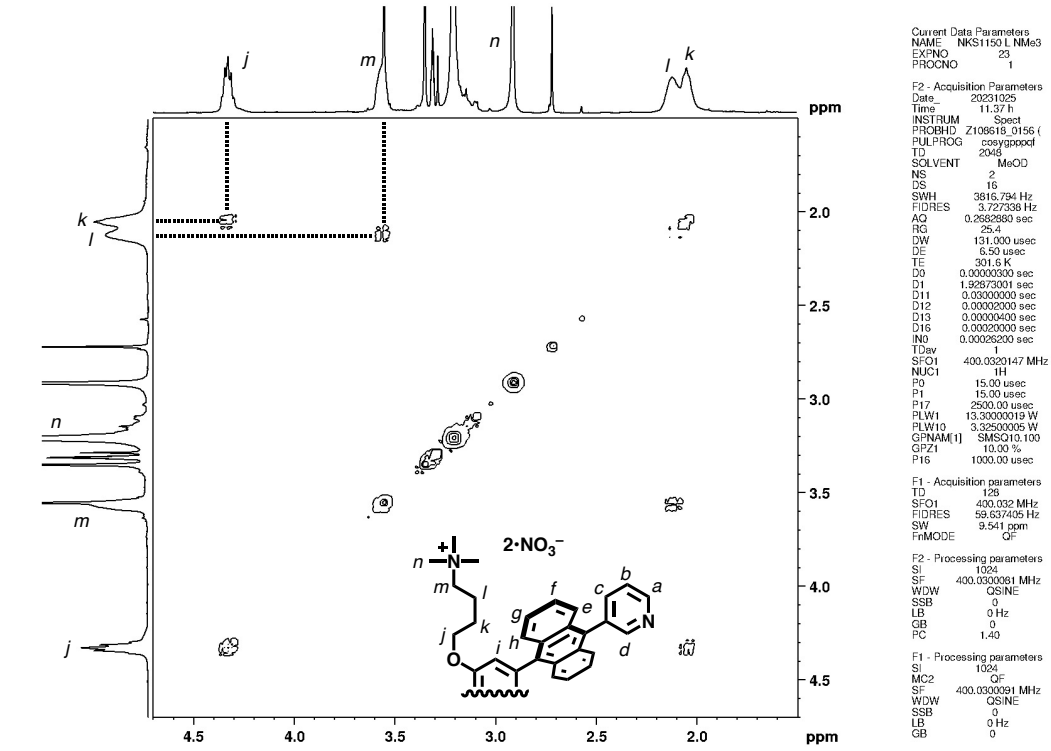

Figure S12. ^{1}H-^{1}H COSY NMR spectrum (400 MHz, CD_3OD, r.t.) of **2**.

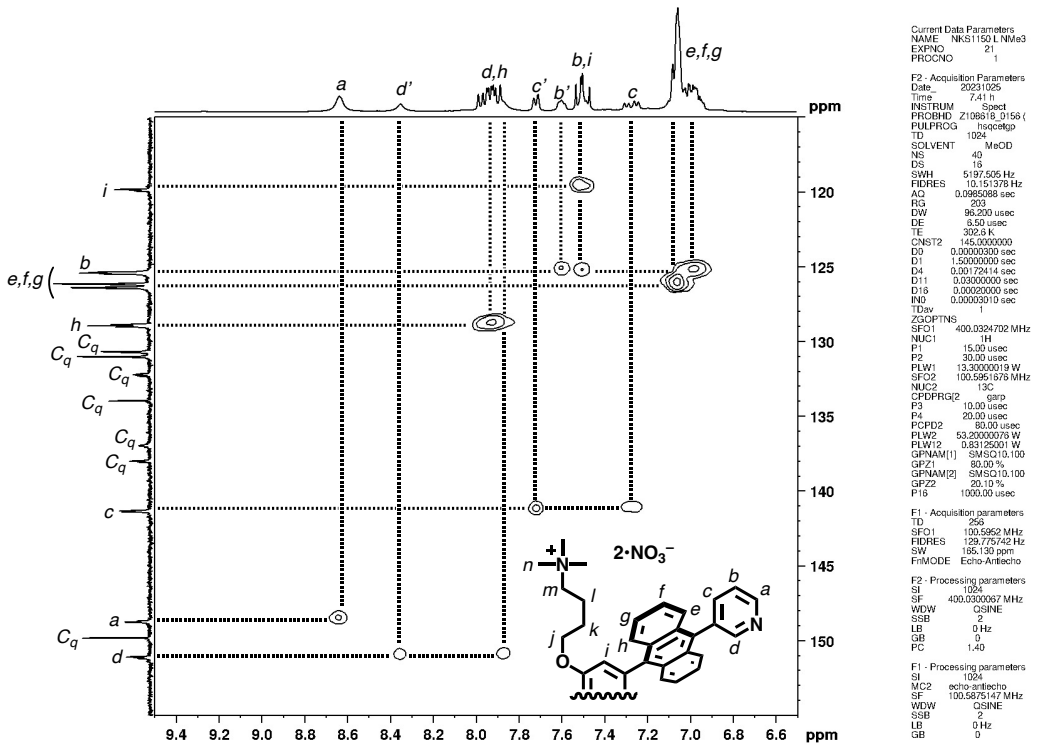

Figure S13a. HSQC NMR spectrum (400 MHz, CD_3OD, r.t.) of **2**.

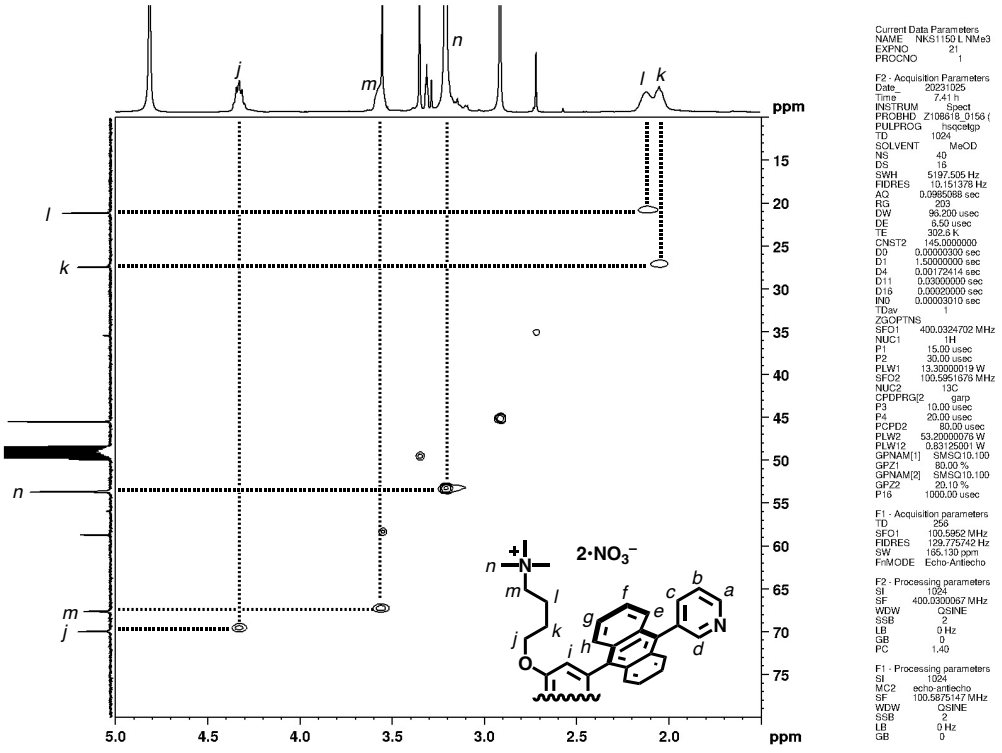

Figure S13b. HSQC NMR spectrum (400 MHz, CD_3OD, r.t.) of **2**.

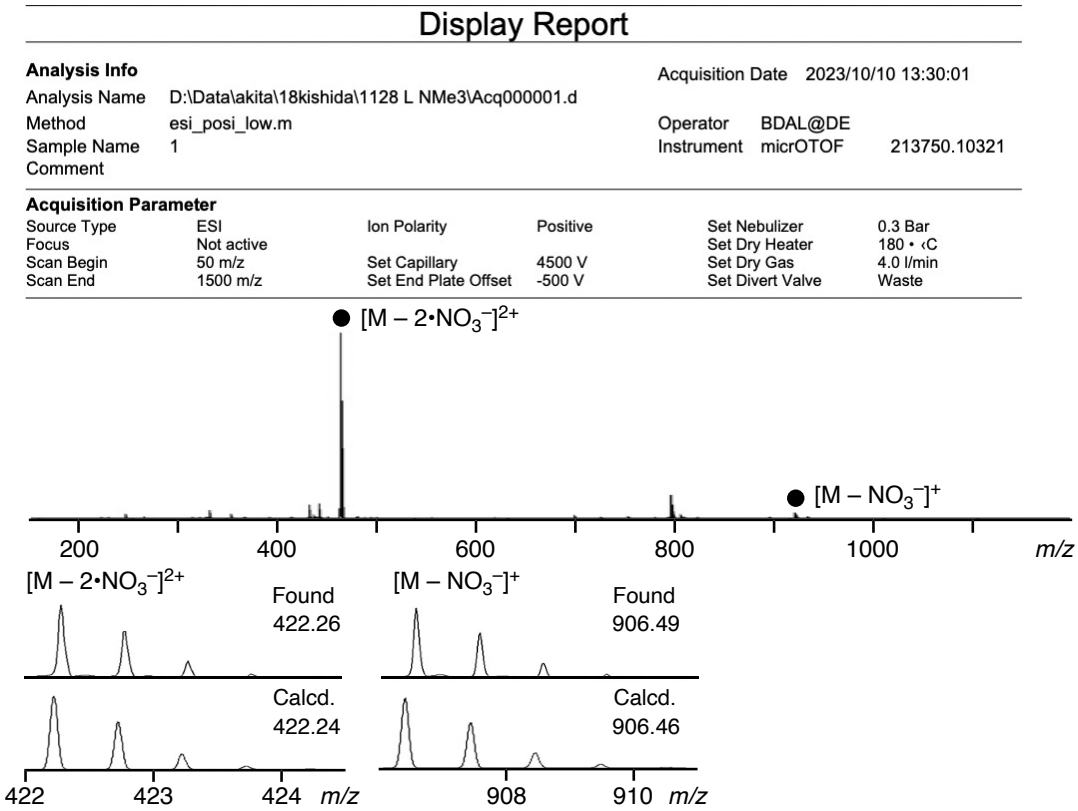

Figure S14. ESI-TOF MS spectrum (CH_3OH) of **2**.

Formation of capsule 1 NKS1157

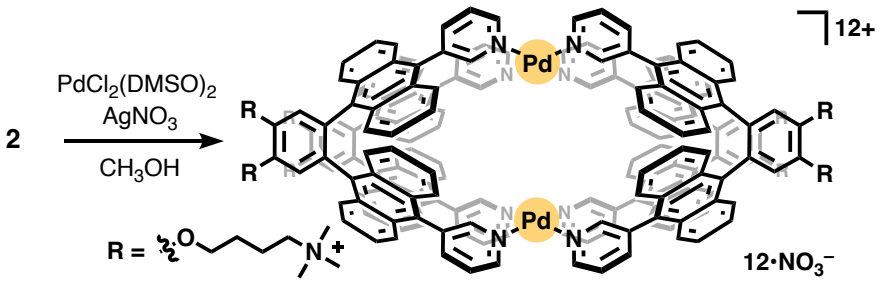

Ligand **2** (30.1 mg, 31.1 μmol), $PdCl_2(DMSO)_2$ (5.45 mg, 16.3 μmol), $AgNO_3$ (5.55 mg, 32.7 μmol), and CH_3OH (2.0 mL) were added to a glass test tube and then the mixture was stirred at 60 ºC for 3 h. After filtration, the crude product was concentrated under reduced pressure. The product was reprecipitated with CH_3OH/acetone and CH_3OH/Et_2O to the resultant solution, capsule **1** was obtained as a yellow solid (25.5 mg, 5.87 μmol, 75%).

^{1}H NMR (500 MHz, CD_3OD, r.t.): δ 8.84 (d, J = 5.0 Hz, 8H), 8.76 (br, 8H), 8.32 (d, J = 8.8 Hz, 8H), 8.19 (d, J = 8.8 Hz, 8H), 8.03-7.97 (m, 16H), 7.51 (dd, J = 7.7, 7.7 Hz, 16H), 7.13 (s, 8H), 7.08 (dd, J = 8.2, 7.7 Hz, 8H), 6.76 (dd, J = 8.2, 7.7 Hz, 8H), 6.67 (d, J = 8.2 Hz, 8H), 6.53 (d, J = 8.2 Hz, 8H), 4.20 (t, J = 4.8 Hz, 16H), 3.52-3.49 (m, 16H), 3.17 (s, 72H), 2.09-2.03 (m, 16H). ^{13}C NMR (125 MHz, $CDCl_3$, r.t.): δ 156.2 (CH), 152.1 (CH), 149.8 (C_q), 146.7 (CH), 139.5 (C_q), 139.2 (C_q), 133.9 (C_q), 131.4 (C_q), 131.3 (C_q), 131 (C_q), 130.5 (C_q), 130.4 (CH), 129.6 (CH), 128.2 (CH), 127.6 (CH), 126.9 (CH), 126.4 (CH), 126 (CH), 125.5 (CH), 125 (CH), 119.3 (CH), 69.7 (CH_2), 67.5 (CH_2), 53.6 (CH_3), 27.3 (CH_2), 21 (CH_2). FT-IR (ATR, cm^{-1}): 2927, 1512, 1480, 1440, 1338, 1242, 1195, 1161, 1088, 1031, 973, 829, 772, 708, 691, 675, 615. ESI-TOF MS (CH_3OH): m/z 557.53 [M – 7•NO_3^-]$^{7+}$, 660.95 [M – 6•NO_3^-]$^{6+}$, 805.34 [M – 5•NO_3^-]$^{5+}$, 1022.47 [M – 4•NO_3^-]$^{4+}$.

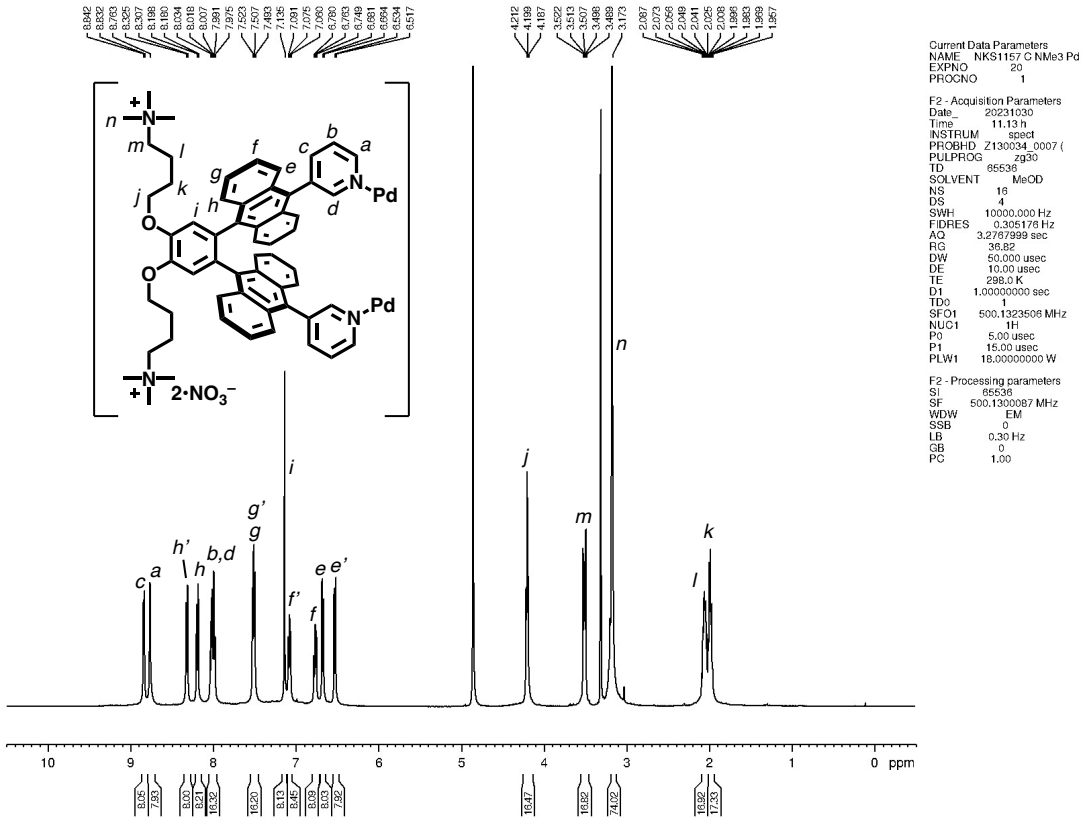

Figure S15. ^{1}H NMR spectrum (500 MHz, CD_3OD, r.t.) of **1**.

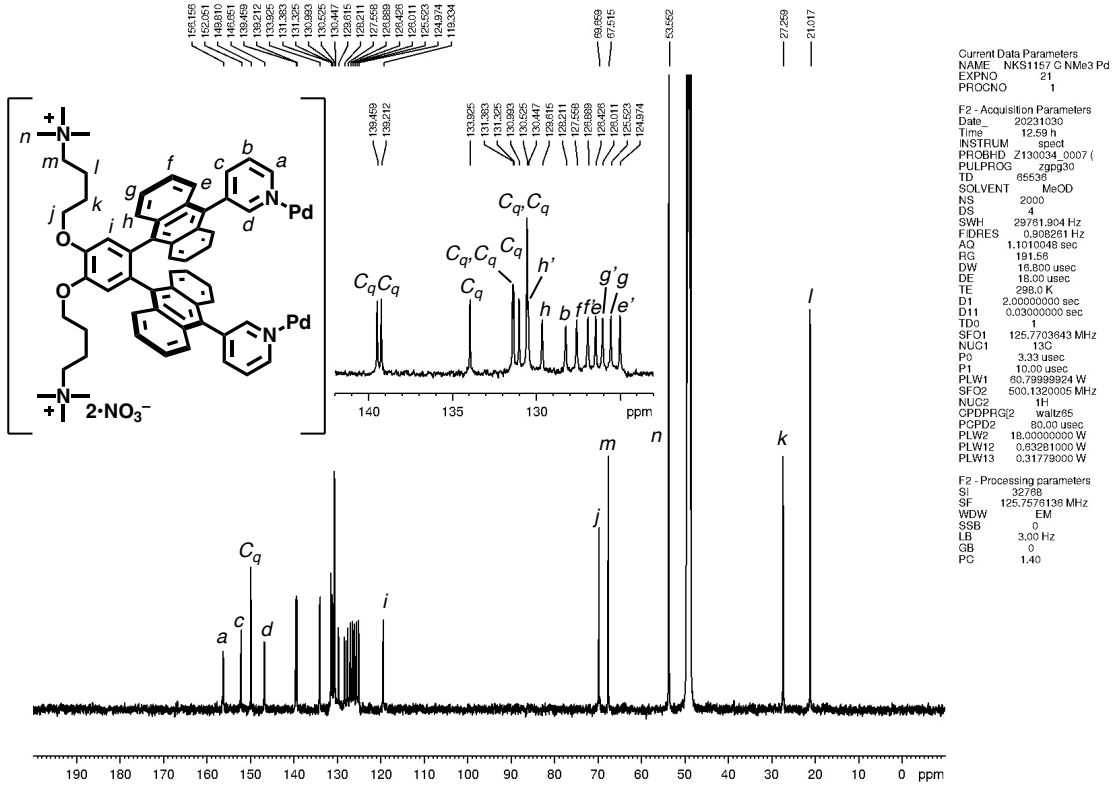

Figure S16. ^{13}C NMR spectrum (125 MHz, CD_3OD, r.t.) of **1**.

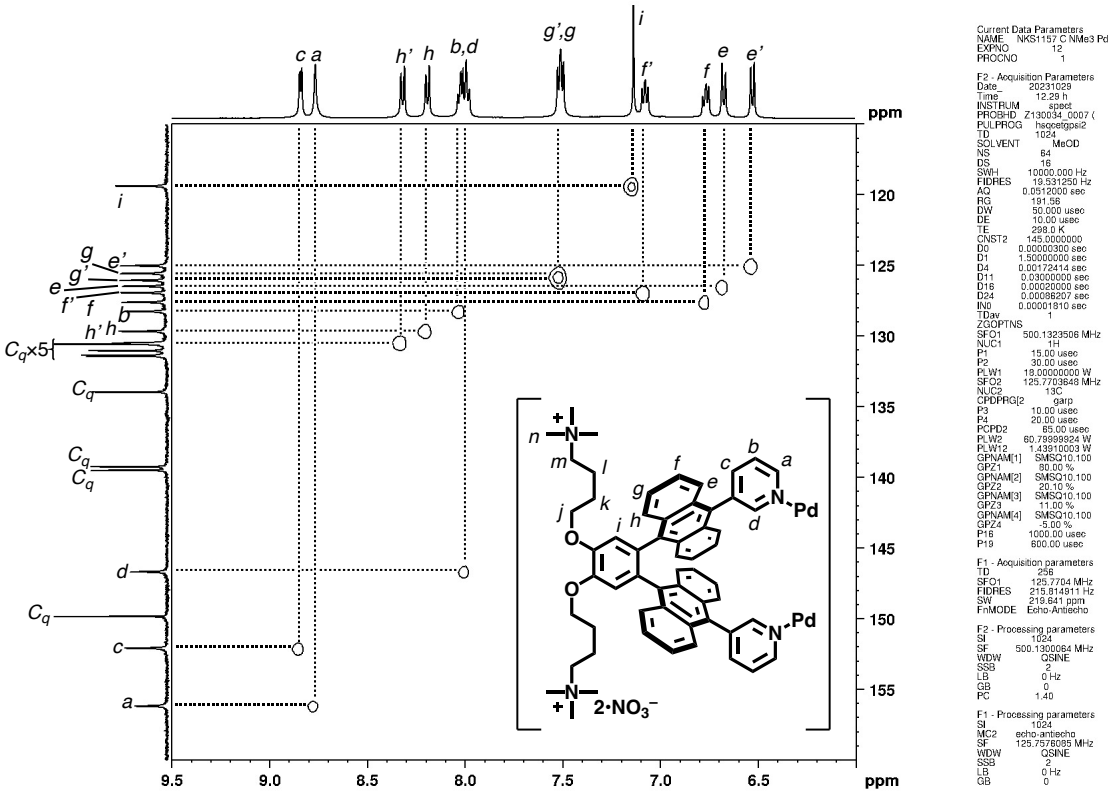

Figure S17. HSQC NMR spectrum (500 MHz, CD_3OD, r.t.) of **1**.

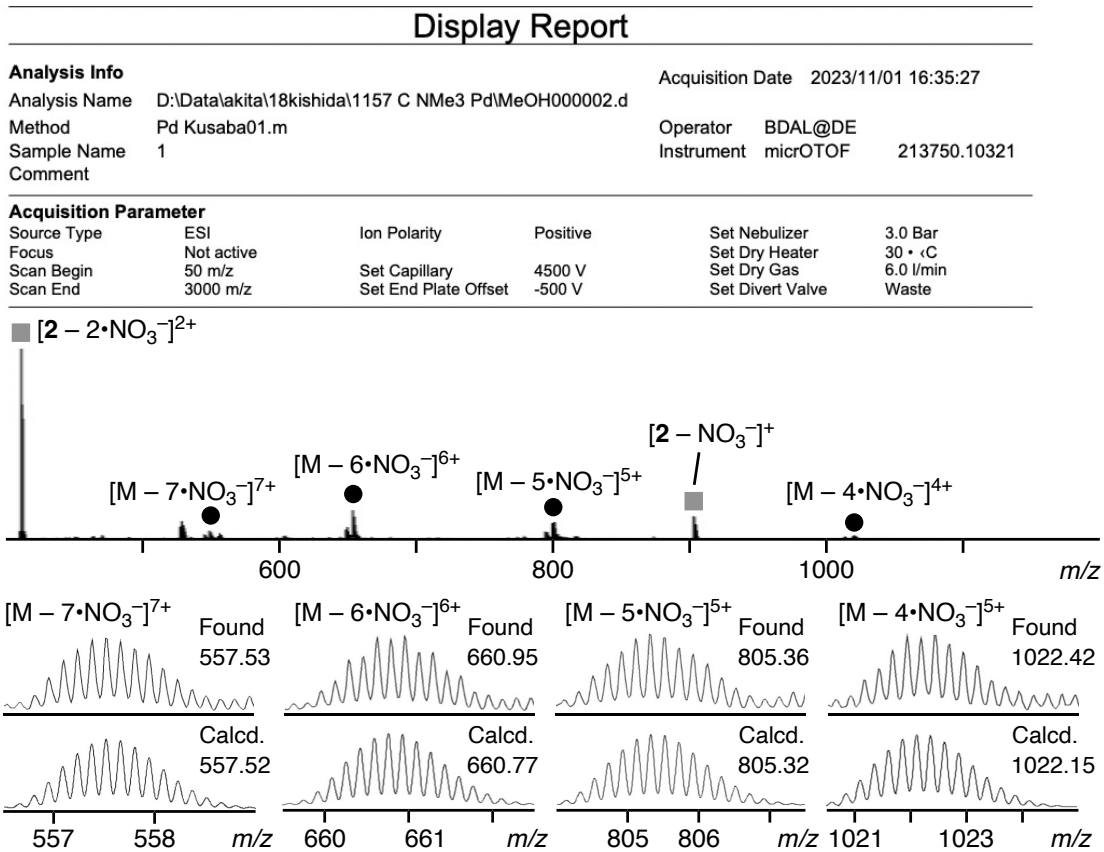

Figure S18. ESI-TOF MS spectrum (CH_3OH) of **1**.

Formation of 1:1 host-guest complexes NKS1161,1164,1171-1173

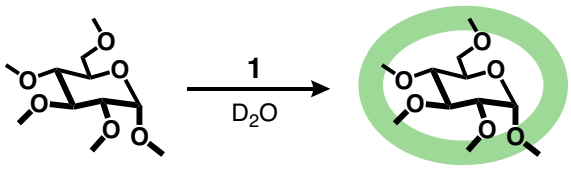

Capsule **1** (0.43 mg, 0.10 μmol), pentamethylated α-D-glucose (**αGlc^{Me}**; 0.050 mg, 0.20 μmol (via a stock solution)), and D_2O (0.5 mL) were added to a glass test tube (7 mL). The mixture was stirred at 80 ºC for 1 h. The quantitative formation of 1:1 host-guest complex **1•αGlc^{Me}** was confirmed by ^{1}H NMR analysis. In the similar way, the quantitative formation of **1•αGal^{Me}**, **1•βGal^{Me}**, and **1•αMan^{Me}** from **1** and the corresponding monosaccharides in D_2O was confirmed by ^{1}H NMR analysis, respectively. Capsule **1** (0.43 mg, 0.10 μmol), a 1:4 mixture of pentamethylated α/β-D-glucose (**α/βGlc^{Me}**; 0.10 mg, 0.41 μmol based on **βGlc^{Me}**), and D_2O (0.5 mL) were added to a glass test tube. The mixture was stirred at 80 ºC for 1 h. The formation of 1:1 host-guest complex **1•βGlc^{Me}** in 95% yield was confirmed by NMR analysis.

1•αGlc^{Me}: ^{1}H NMR (500 MHz, D_2O, r.t.): δ 8.92 (d, J = 5.3 Hz, 4H), 8.88 (d, J = 5.3 Hz, 4H), 8.43 (m, 8H), 8.34 (m, 8H), 8.25-8.17 (m, 16H), 8.05 (s, 4H), 8.03 (s, 4H), 7.65 (m, 16H), 7.22 (s, 4H), 7.22 (dd, J = 7.5, 7.5 Hz, 8H), 7.18 (s, 4H), 6.98 (dd, J = 7.7, 7.7 Hz, 4H), 6.69 (d, J = 9.2 Hz, 4H), 6.66 (dd, J = 7.2, 7.2 Hz, 4H), 6.61 (d, J = 8.6 Hz, 4H), 6.54 (d, J = 8.5 Hz, 4H), 6.53 (d, J = 8.5 Hz, 4H), 4.26 (m, 16H), 3.42 (m, 16H), 3.12 (s, 32H), 3.12 (s, 32H), 2.81 (m, 1H), 2.55 (d, J = 3.2 Hz, 1H), 2.38-2.34 (m, 2H), 2.01-1.95 (m, 32H), 1.86 (m, 1H), 1.31 (dd, J = 9.0, 9.0 Hz, 1H), 0.68 (d, J = 10.5 Hz, 1H), 0.00 (s, 3H), –0.31 (s, 3H), –0.55 (s, 3H), –0.83 (s, 3H), –0.87 (s, 3H).

1•βGlc^{Me}: ^{1}H NMR (500 MHz, D_2O, r.t.): δ 8.91 (m, 4H), 8.87 (d, J = 5.7 Hz, 4H), 8.84 (d, J = 5.8 Hz, 4H), 8.42 (m, 8H), 8.34-8.26 (m, 16H), 8.19 (m, 8H), 8.10 (s, 2H), 8.07 (s, 4H), 7.92 (s, 2H), 7.64 (m, 16H), 7.23-7.20 (m, 16H), 6.98 (dd, J = 8.2, 8.2 Hz, 1.8H), 6.94 (dd, J = 7.2, 9.0 Hz, 2.2H), 6.82 (dd, J = 7.5, 7.5 Hz, 1.8H), 6.77 (dd, J = 7.6, 7.6 Hz, 2.2H), 6.71 (d, J = 8.8 Hz, 1.8H), 6.66 (d, J = 8.9 Hz, 2.2H), 6.61-6.54 (m, 8H), 4.26 (m, 16H), 3.41 (m, 16H), 3.12 (s, 72H), 2.75 (m, 1H), 2.55 (d, J = 4.1 Hz, 1H), 2.37 (m, 1H), 2.00–1.96 (m, 32H), 1.68 (m, 0.5H), 1.44 (m, 0.5H), 1.34 (m, 0.5H), 1.15 (m, 0.5H), 1.06 (m, 0.5H), 0.76 (m, 0.5H), 0.50 (m, 0.5H), 0.45 (m, 0.5H), –0.11 (s, 1.6H), –0.14 (s, 1.4H), –0.29 (s, 1.4H), –0.44 (s, 1.6H), –0.46 (s, 1.6H), –0.67 (s, 3H), –0.70 (s, 1.4H), –0.83 (s, 1.6H), –0.86 (s, 1.4H).

1•αGal^{Me}: ^{1}H NMR (500 MHz, D_2O, r.t.): δ 8.97-8.94 (m, 4H), 8.91 (d, J = 5.5 Hz, 3.1H), 8.87 (d, J = 5.8 Hz, 0.9H), 8.48-8.41 (m, 8H), 8.33-8.67 (m, 27.1H), 8.06 (s, 3.1H), 8.03 (s, 0.9H), 7.97 (s, 0.9H), 7.72–7.63 (m, 12.9), 7.59 (dd, J = 7.7, 7.7 Hz, 3.1H), 7.25 (m, 8H), 7.21 (s, 0.9H), 7.20 (s, 3.1H), 7.18 (s, 0.9H), 7.15 (s, 3.1H), 6.99 (dd, J = 6.8, 8.0 Hz, 0.9H), 6.89 (dd, J = 7.1, 8.3 Hz, 3.1H), 6.75-6.70 (m, 1.8H), 6.65-6.52 (m, 15.1H), 6.49 (d, J = 9.0 Hz, 31.H), 4.24 (m, 16H), 3.41 (m, 16H), 3.11 (s, 32H), 3.11 (s, 32H), 2.82 (d, J = 9.3 Hz, 1H), 2.66 (d, J = 3.5 Hz, 1H), 2.00-1.94 (m, 32H), 1.34 (dd, J = 4.1, 10.1 Hz, 1H), 1.22 (d, J = 3.4 Hz, 1H), 0.12 (s, 2.3H), 0.09 (s, 0.7H), –0.26 (s, 0.7H), –0.29 (d, J = 12.0 Hz, 1H), –0.38 (s, 0.7H), –0.48 (s, 0.7H), –0.82 (s, 2.3H), –0.87 (s, 2.3H), –0.99 (s, 2.3H), –1.08 (s, 2.3H), –1.19 (s, 0.7H).

1•βGal^{Me}: ^{1}H NMR (500 MHz, D_2O, r.t.): δ 8.91-8.88 (m, 8H), 8.46-8.40 (m, 8H), 8.35-8.27 (m, 16H), 8.19 (m, 8H), 8.09 (s, 2.5H), 8.03 (s, 1.5H), 7.99 (s, 1.5H), 7.96 (s, 2.5H), 7.66 (m, 16H), 7.26-7.19 (m, 16H), 6.91 (dd, J = 6.9, 8.3 Hz, 3H), 6.86-6.81 (m, 5H), 6.65-6.55 (m, 16H), 4.25 (m, 16H), 3.43 (m, 16H), 3.12 (s, 72H), 2.16-2.13 (m, 3H), 2.01-1.96 (m, 32H), 1.72 (m, 1H), 1.28 (dd, J = 4.7, 7.0 Hz, 1H), 1.20 (m, 0.3H), 1.16 (m, 0.7H), 0.31 (d, J = 7.7 Hz, 1.1H), –0.02 (s, 1.9H), –0.12 (s, 1.1H), –0.17 (s, 1.9H), –0.28 (s, 1.9H), –0.35 (s, 1.1H), –0.49 (s, 1.1H), –0.55 (s, 1.9H), –0.80 (s, 1.1H), –0.92 (s, 1.1H), –1.06 (s, 1.9H).

1•αMan^{Me}: ^{1}H NMR (500 MHz, D_2O, r.t.): δ 8.90 (m, 8H), 8.45 (d, J = 8.7 Hz, 4H), 8.41 (d, J = 8.9 Hz, 4H), 8.35-8.27 (m, 16H), 8.20 (m, 8H), 8.06 (s, 0.5H), 8.03 (s, 3.5H), 7.99 (s, 4H), 7.64-7.58 (m, 16H), 7.23-7.18 (m, 16H), 6.93 (dd, J = 7.1, 9.0 Hz, 0.5H), 6.84 (dd, J = 7.3, 7.9 Hz, 3.5H), 6.72 (dd, J = 6.7, 8.5 Hz, 3.5H), 6.69-6.50 (m, 16.5H), 4.25 (t, J = 6.0 Hz, 16H), 3.42 (m, 16H), 3.11 (s, 72H), 2.38 (m, 1H), 2.01-1.94 (m, 32H), 1.86 (m, 1H), 1.81 (m, 1H), 1.63-1.17 (m, 2H), 0.70 (d, J = 10.8 Hz, 1H), 0.62 (d, J = 3.5 Hz, 1H), 0.19 (s, 2.6H), –0.14 (s, 0.4H), –0.29 (s, 2.6H), –0.35 (s, 0.4H), –0.40 (s, 2.6H), –0.46 (s, 2.6H), –0.50 (s, 2.6H), –0.62 (s, 0.4H), –0.73 (s, 0.4H), –0.84 (s, 0.4H).

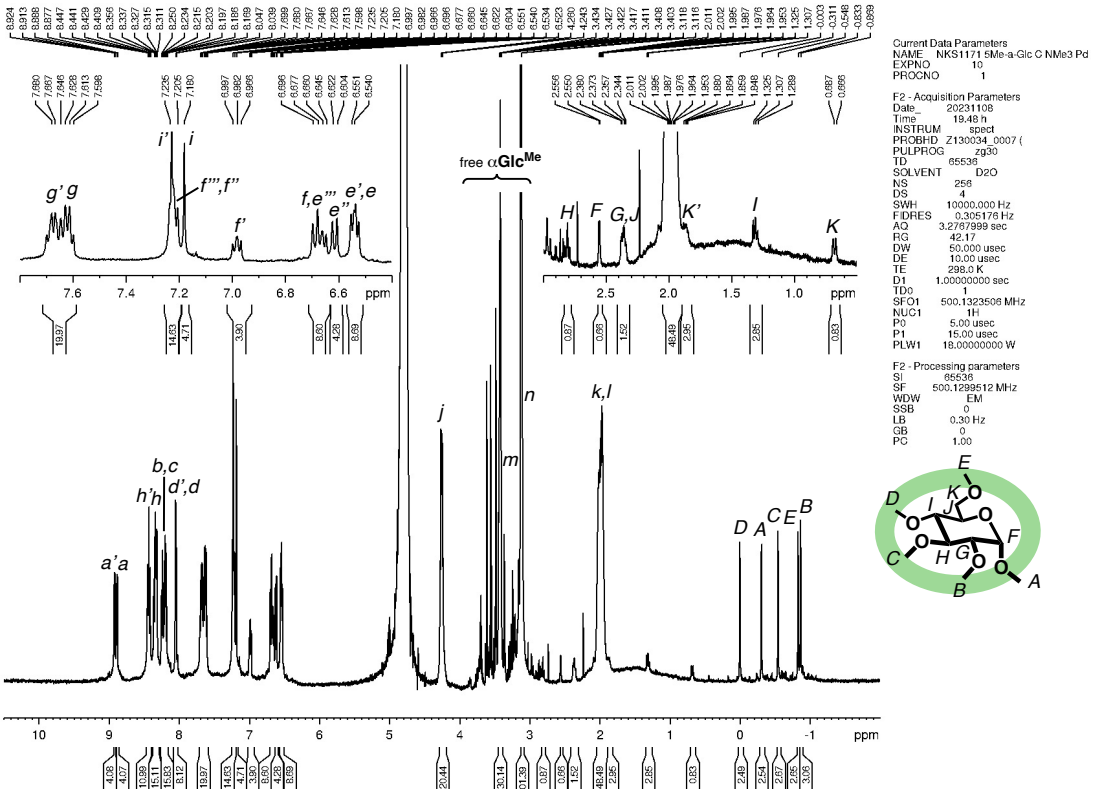

Figure S19a. ^{1}H NMR spectrum (500 MHz, D_2O, r.t.) of **1•αGlc^{Me}**.

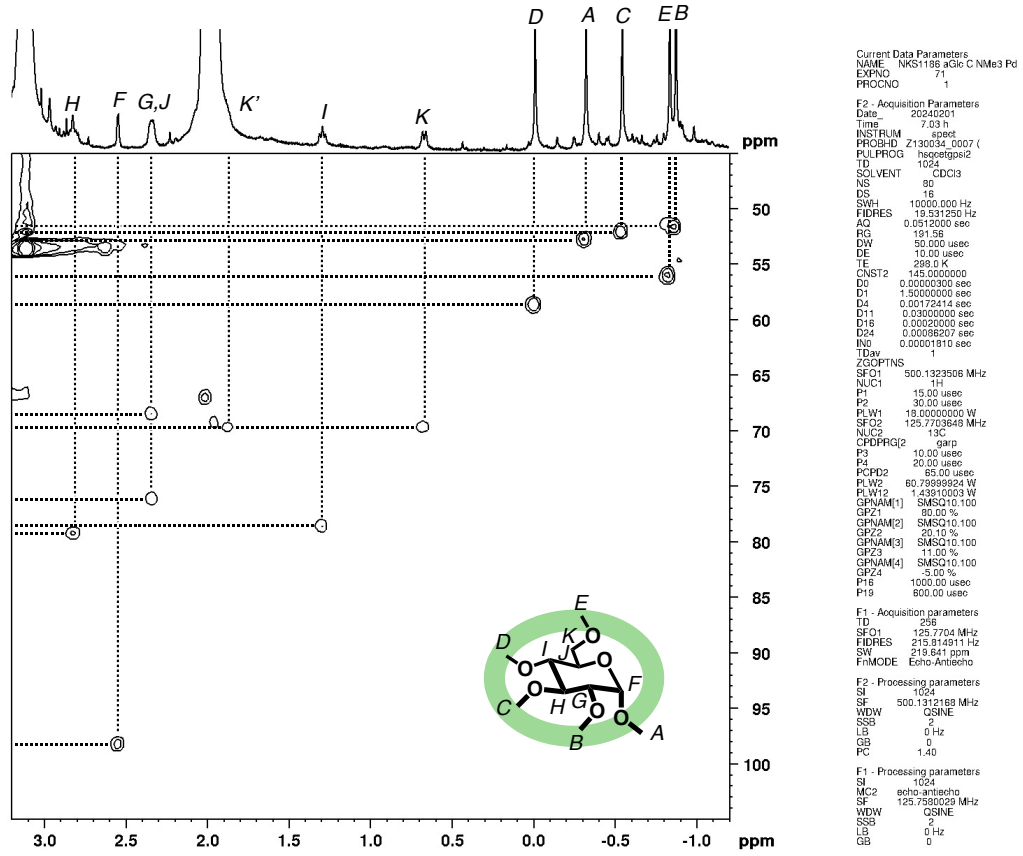

Figure S19b. HSQC NMR spectrum (500 MHz, D_2O, r.t.) of **1•αGlc^{Me}**.

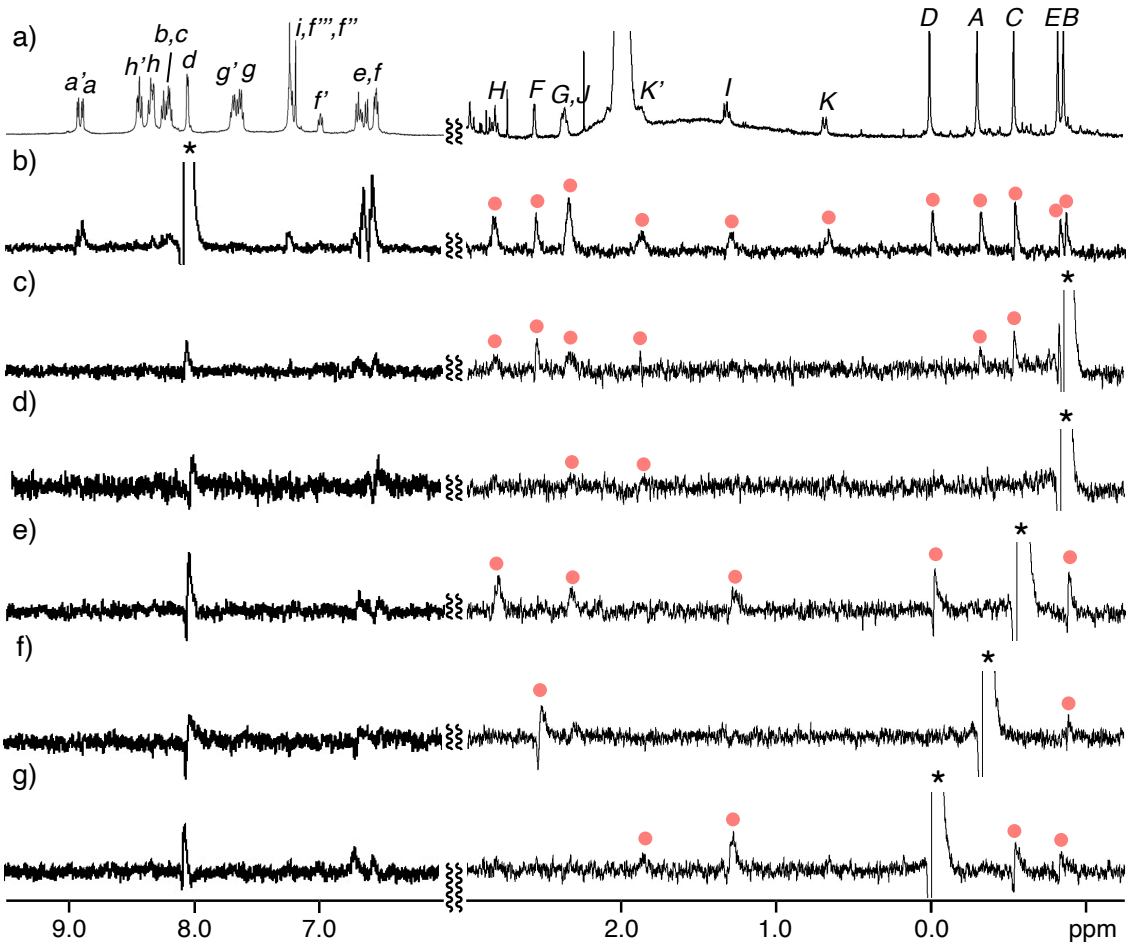

Figure S19c. 1D-NOESY spectra (500 MHz, D_2O, r.t.) of **1•αGlc^{Me}** a) without irradiation, and with irradiation at b) 8.04, c) –0.88, d) –0.84, e) –0.55, f) –0.33, and g) –0.01 ppm.

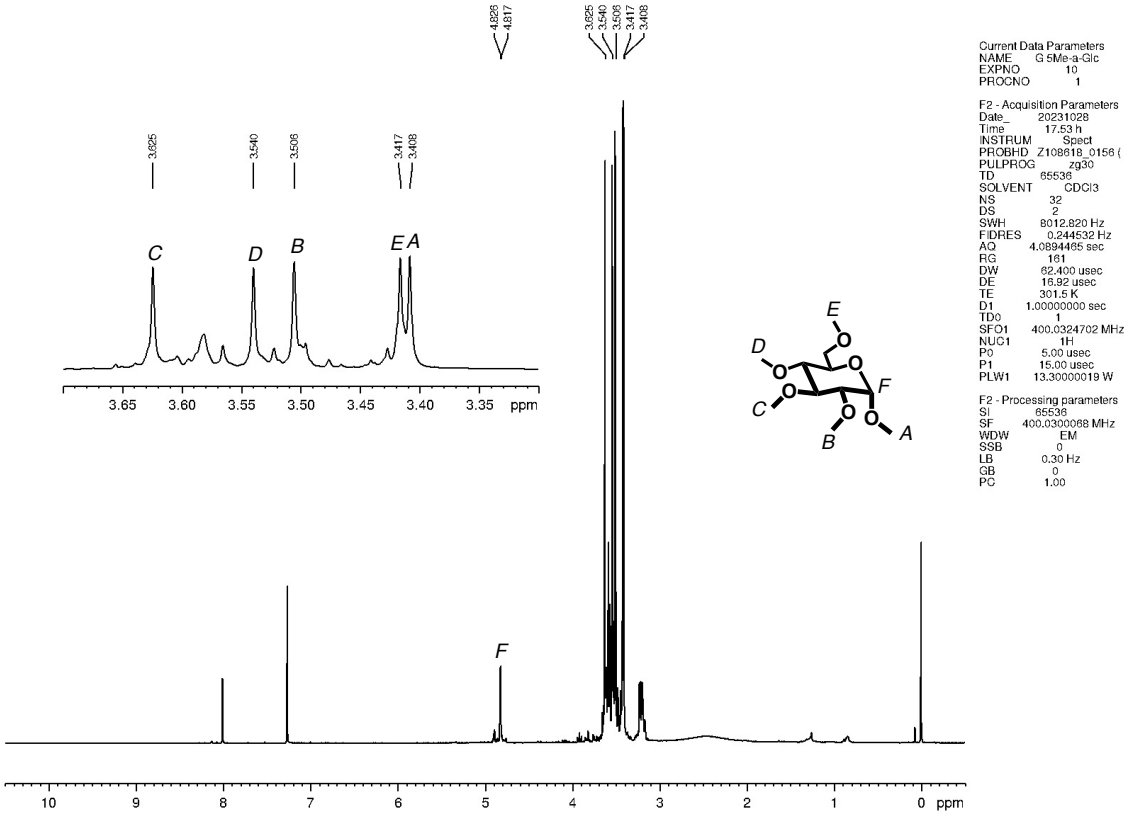

Figure S19d. ^{1}H NMR spectrum (400 MHz, $CDCl_3$, r.t.) of **αGlc^{Me}**.

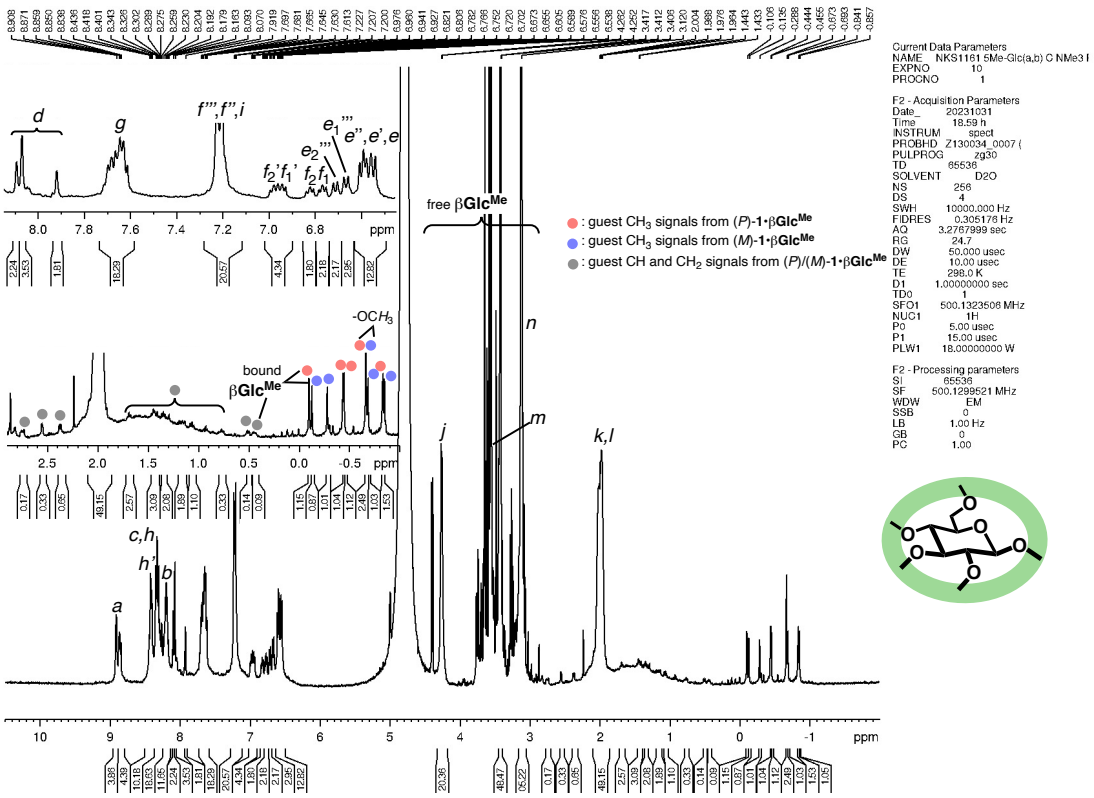

Figure S20. ^{1}H NMR spectrum (500 MHz, D_2O, r.t.) of **1•βGlc^{Me}**.

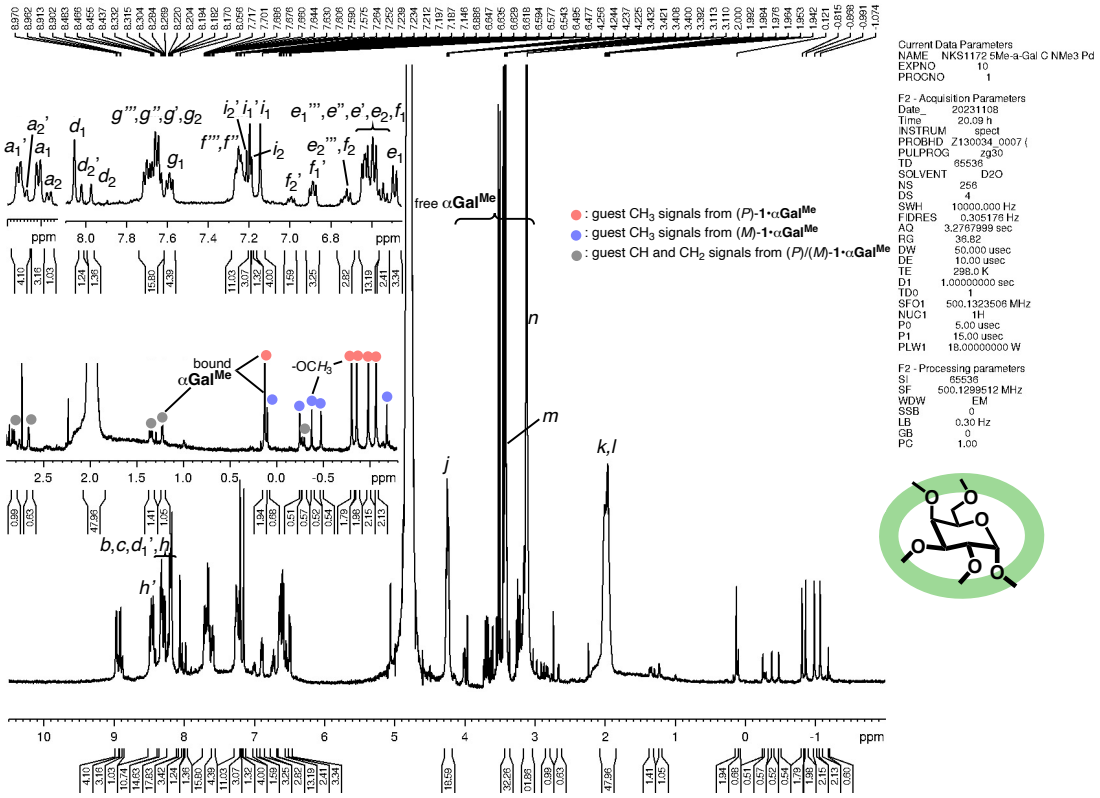

Figure S21. ^{1}H NMR spectrum (500 MHz, D_2O, r.t.) of **1•αGal^{Me}**.

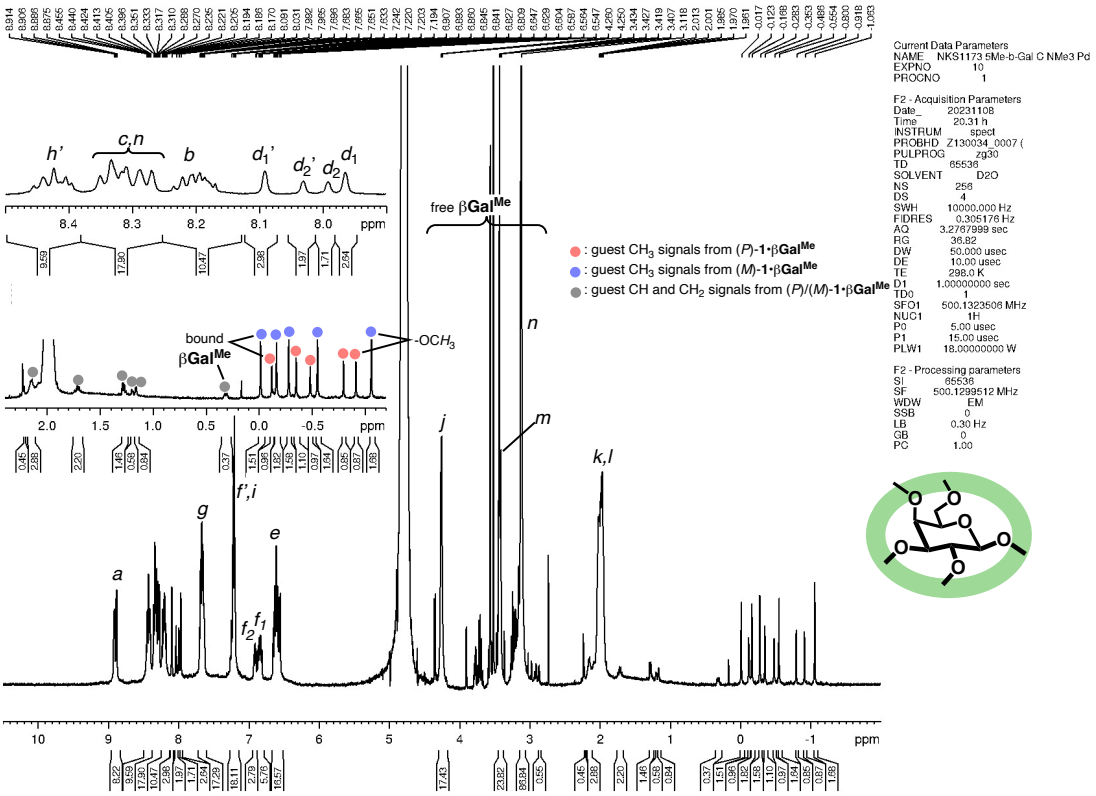

Figure S22. ^{1}H NMR spectrum (500 MHz, D_2O, r.t.) of **1•βGal^{Me}**.

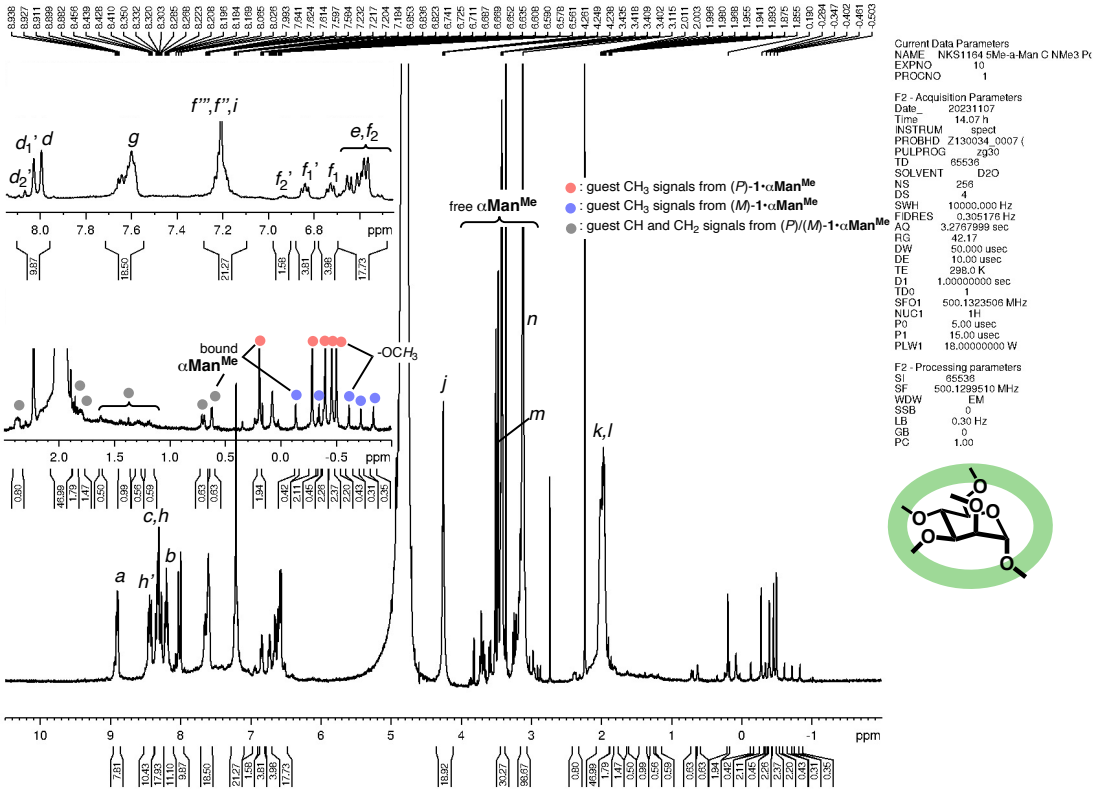

Figure S23. ^{1}H NMR spectrum (500 MHz, D_2O, r.t.) of **1•αMan^{Me}**.

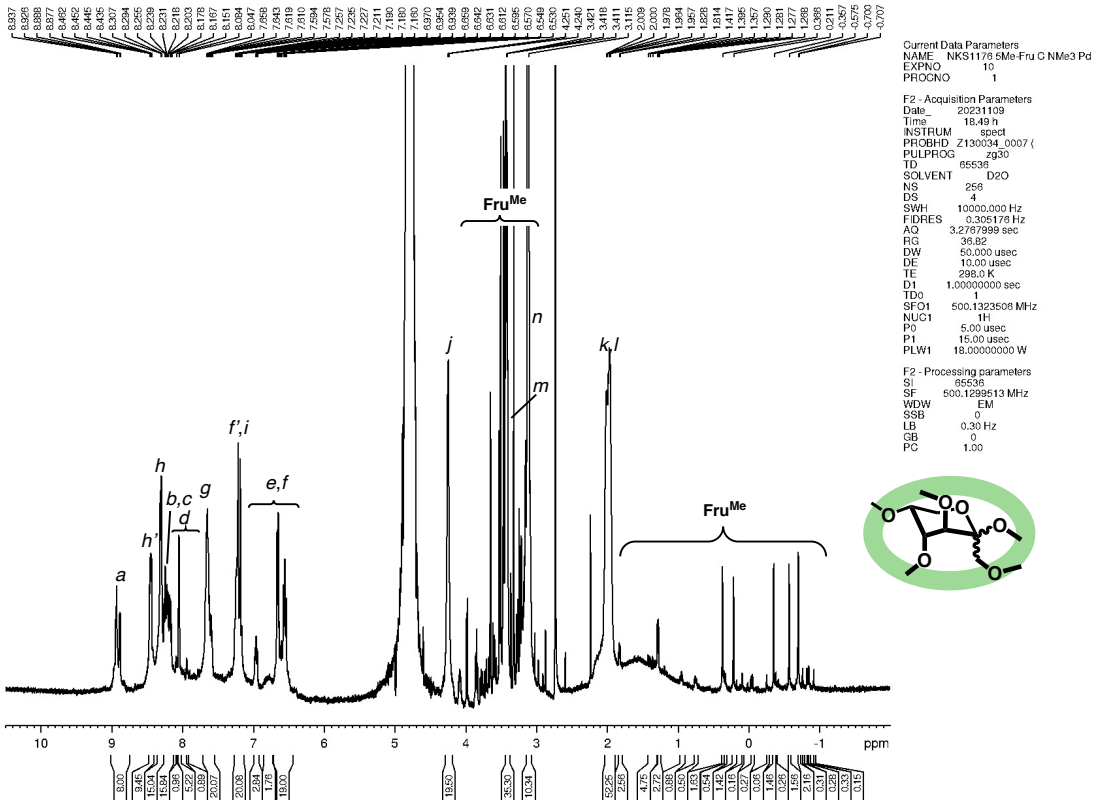

Figure S24. ^{1}H NMR spectrum (500 MHz, D_2O, r.t.) of **1•Fru^{Me}**.

Formation of 1”•αGlc^{Me} NKS1182

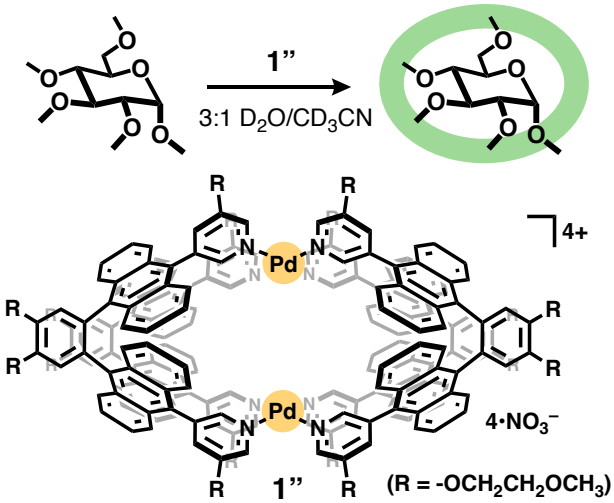

For the MS analysis, capsule **1”** (0.43 mg, 0.10 μmol), **αGlc^{Me}** (1.3 mg, 5.0 μmol), and 3:1 D_2O/CD_3CN (0.5 mL) were added to a glass test tube. The mixture was stirred at 80 ºC for 1 h. The formation of 1:1 host-guest complex **1”•αGlc^{Me}** in 65% yield was confirmed by NMR analysis. The product solution was concentrated under reduced pressure and washed with water to remove excess **αGlc^{Me}**. The structure of the 1:1 host-guest complex was confirmed by MS analysis in methanol.

ESI-TOF MS (CH_3OH): *m/z* 996.61 [**1”•αGlc^{Me}** – 4•NO_3^-]$^{4+}$, 1349.15 [**1”•αGlc^{Me}** – 3•NO_3^-]$^{3+}$, 2055.22 [**1”•αGlc^{Me}** – 2•NO_3^-]$^{2+}$.

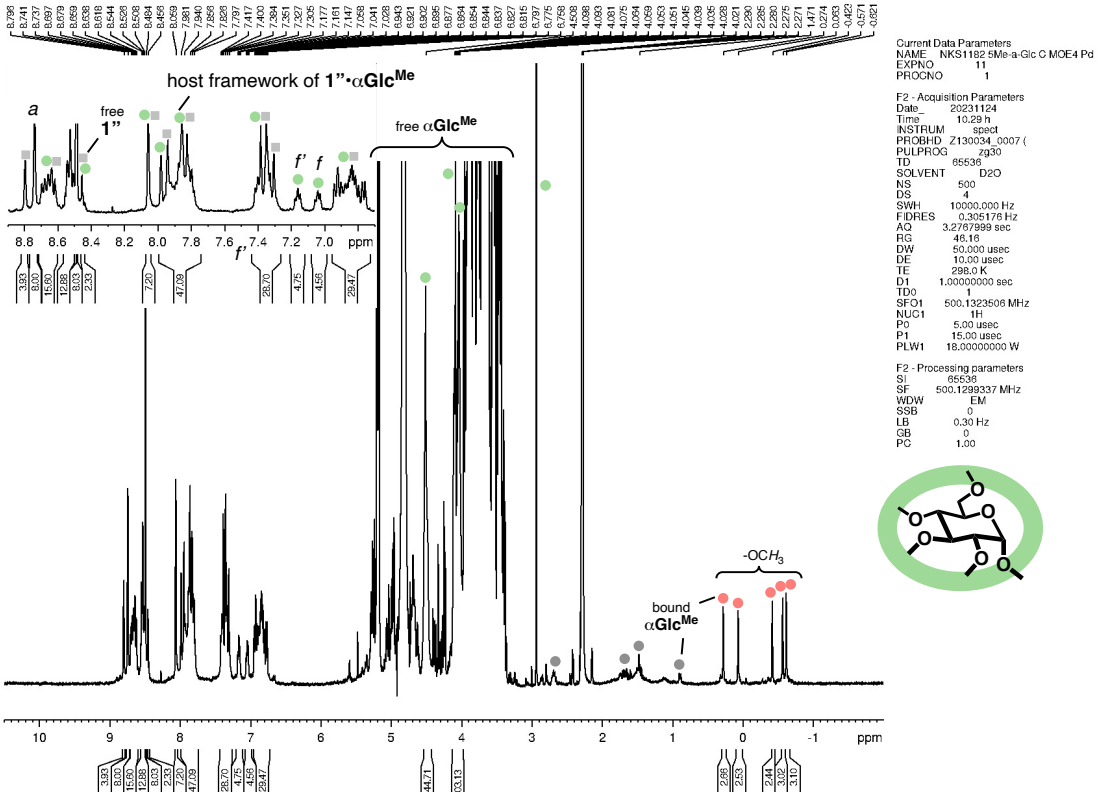

Figure S25. ^{1}H NMR spectrum (500 MHz, 3:1 D_2O/CD_3CN, r.t.) of **1”•αGlc^{Me}**.

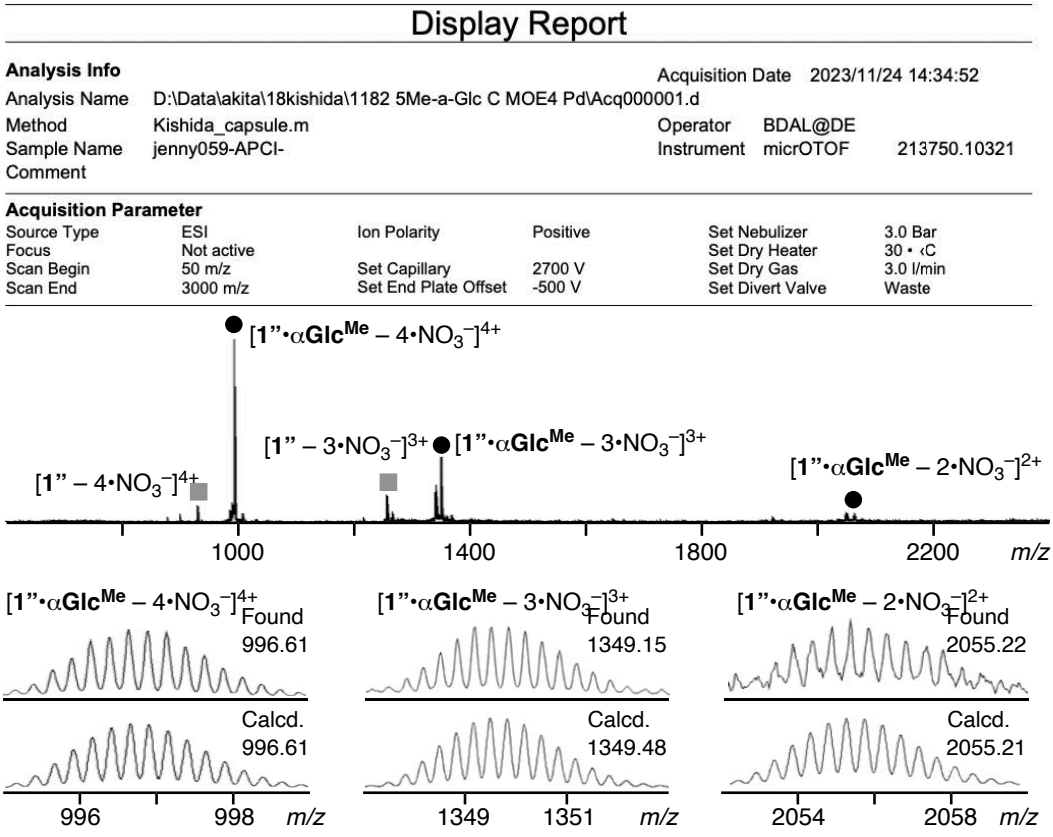

Figure S26. ESI-TOF MS spectrum (CH_3OH) of **1”•αGlc^{Me}**.

Binding constant of 1•βGlc^{Me} NKS1194

Capsule **1** (0.34 mg, 0.078 μmol), 1:4 **α/βGlc^{Me}** mixture (0.10 mg, 0.40 μmol based on **βGlc^{Me}**), and D_2O (0.5 mL) were added to a glass test tube. The mixture was stirred at 80 ºC for 1 h. The product was concentrated under reduced pressure and reprecipitated with CH_3OH/Et_2O to afford **1•βGlc^{Me}** as a yellow solid (0.29 mg, 0.064 μmol, 81%). The obtained host-guest complex was redissolved in D_2O. **1•βGlc^{Me}** is stable enough even under high dilution conditions (~2.5 μM). The exact binding constant (K_a) could not be estimated by the NMR measurement because the proton signals derived from empty **1** and free **βGlc^{Me}** (less than 5%) were not observed under the conditions. Thus, the K_a value (= [**1•βGlc^{Me}**]/([**1**]•[**βGlc^{Me}**])) was roughly estimated to be $>10^8$ M^{-1}.[S4, S5]

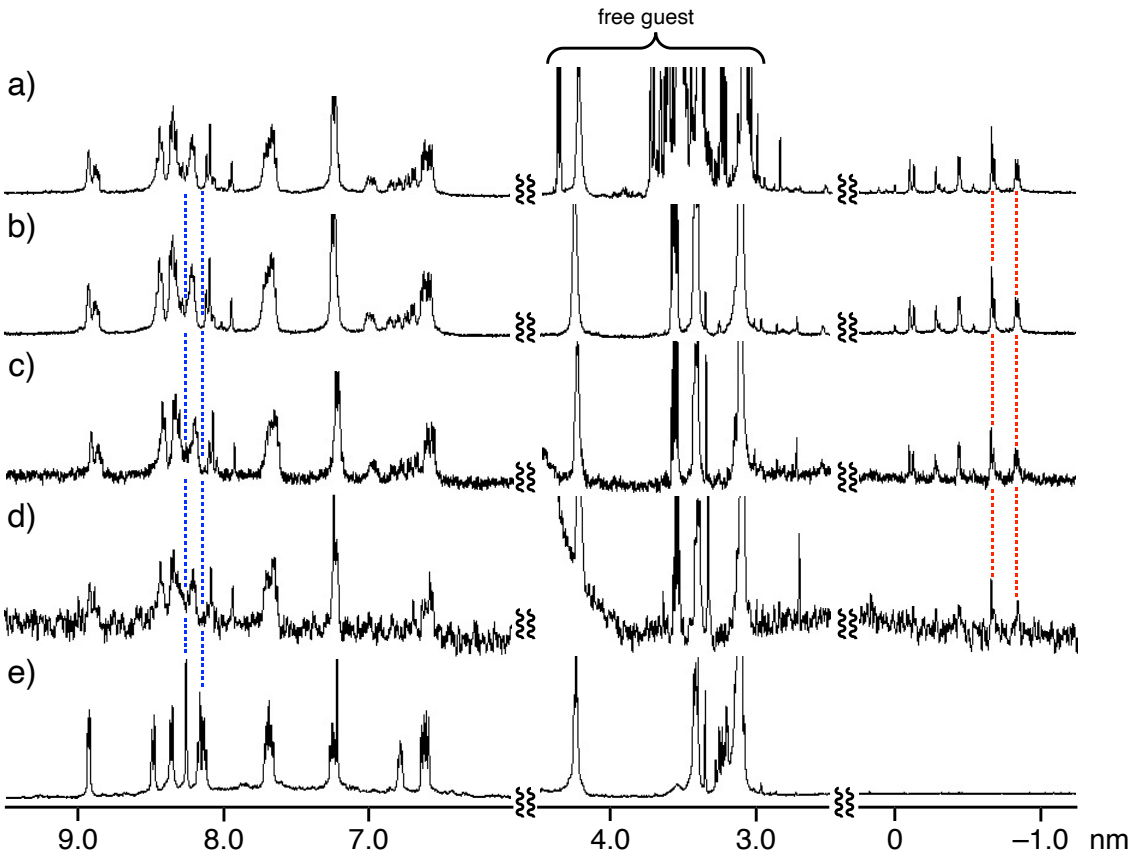

Figure S27. a) ^1H NMR spectrum (500 MHz, D_2O, r.t.) of **1•βGlc^{Me}** before isolation. Concentration-dependent ^1H NMR spectra (500 MHz, D_2O, r.t.) of isolated **1•βGlc^{Me}** at b) 130 μM, c) 13 μM, and d) 2.5 μM. e) ^1H NMR spectrum (500 MHz, D_2O, r.t.) of empty capsule **1** (red dash lines: bound **βGlc^{Me}**, blue dash lines: empty **1**).

Competitive binding experiments NKS1170,1174,1177,1189,1190

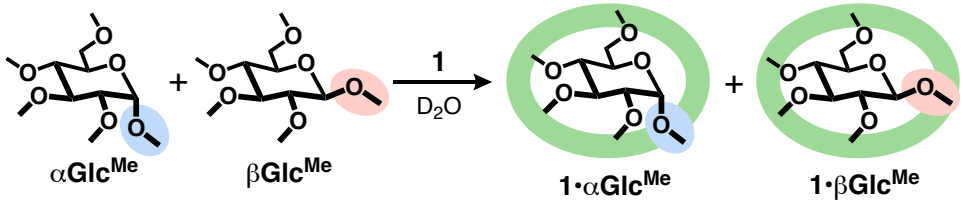

Capsule **1** (0.43 mg, 0.10 μmol), **αGlc^{Me}** (50 μg, 0.20 μmol (via a stock solution)), **βGlc^{Me}** (50 μg, 0.20 μmol (via a stock solution)), and D_2O (0.5 mL) were added to a glass test tube. The mixture was stirred at 80 ºC for 10 min. The formation and product ratio of **1•αGlc^{Me}** and **1•βGlc^{Me}** (19:81) were confirmed by ^{1}H NMR analysis. Various binding experiments were examined in the same way. Similarly, capsule **1** (0.43 mg, 0.10 μmol), **αGlc^{Me}** (50 μg, 0.20 μmol), **βGlc^{Me}** (50 μg, 0.20 μmol), and D_2O (0.5 mL) were added to a glass test tube. The mixture was stirred at 40 ºC for 2 h. The formation and product ratio of **1•αGlc^{Me}** and **1•βGlc^{Me}** (18:82) were confirmed by ^{1}H NMR analysis.

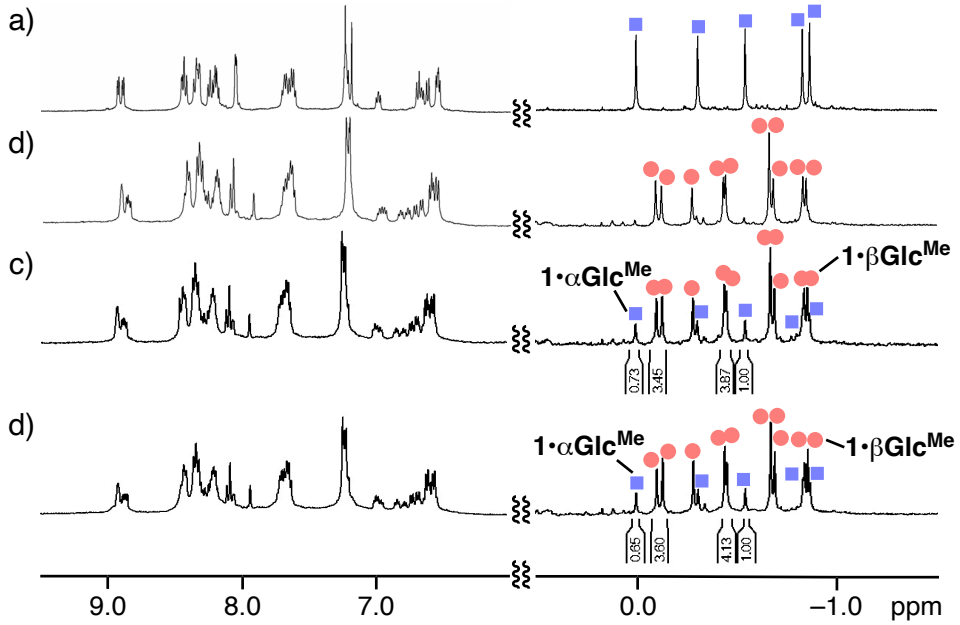

Figure S28. Competitive binding experiment of **1** with **αGlc^{Me}** and **βGlc^{Me}** in water. ^{1}H NMR spectra (500 MHz, D_2O, r.t.) of a) **1•αGlc^{Me}**, b) **1•βGlc^{Me}**, and products after mixing **αGlc^{Me}**, **βGlc^{Me}**, and **1** at c) 80 ºC and d) 40 ºC.

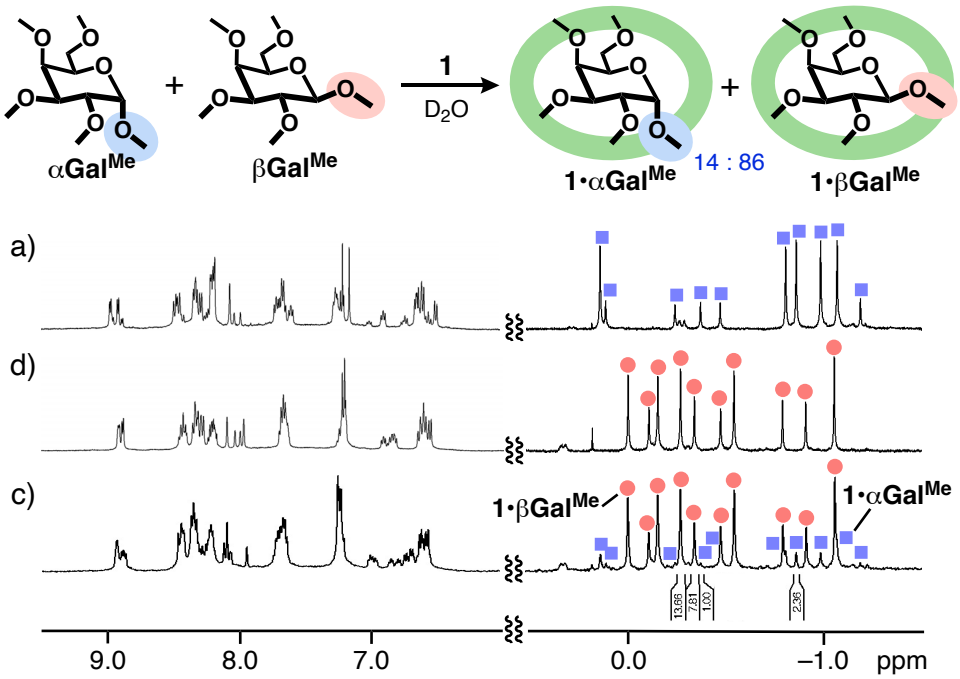

Figure S29. Competitive binding experiment of **1** with **αGal^{Me}** and **βGal^{Me}** in water. ^{1}H NMR spectra (500 MHz, D_2O, r.t.) of a) **1•αGal^{Me}**, b) **1•βGal^{Me}**, and c) products after mixing **αGal^{Me}**, **βGal^{Me}**, and **1**.

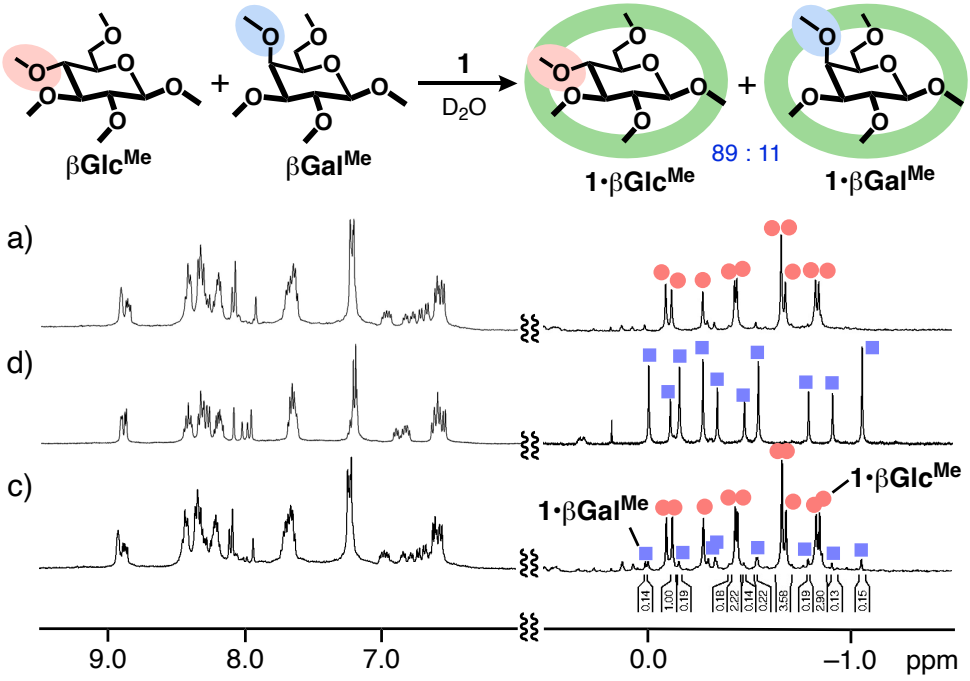

Figure S30. Competitive binding experiment of **1** with **βGlc^{Me}** and **βGal^{Me}** in water. ^{1}H NMR spectra (500 MHz, D_2O, r.t.) of a) **1•βGlc^{Me}**, b) **1•βGal^{Me}**, and c) products after mixing **βGlc^{Me}**, **βGal^{Me}**, and **1**.

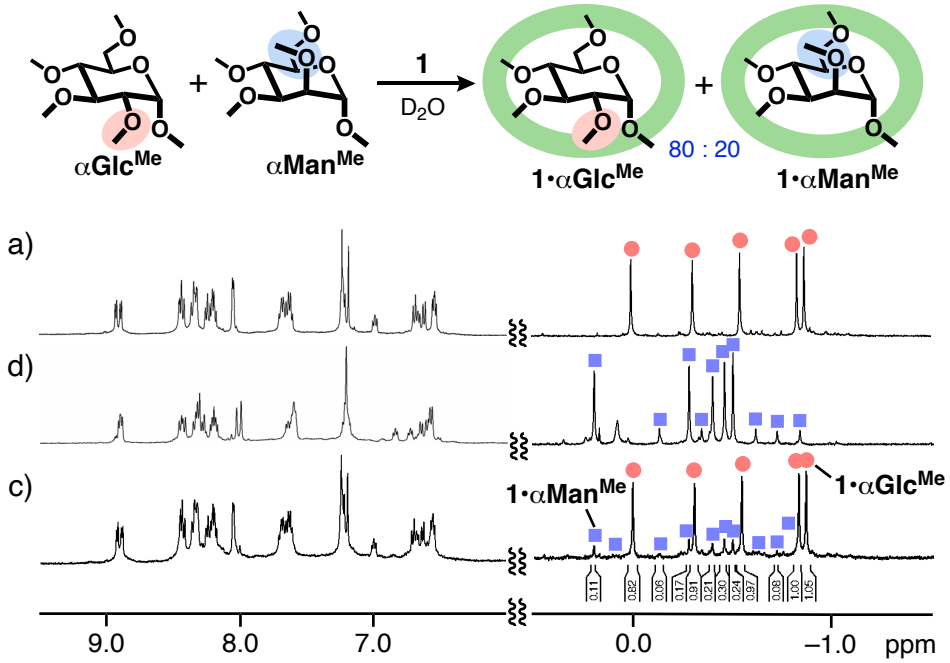

Figure S31. Competitive binding experiment of **1** with **αGlc^{Me}** and **αMan^{Me}** in water. ^{1}H NMR spectra (500 MHz, D_2O, r.t.) of a) **1•αGlc^{Me}**, b) **1•αMan^{Me}**, and c) products after mixing **αGlc^{Me}**, **αMan^{Me}**, and **1**.

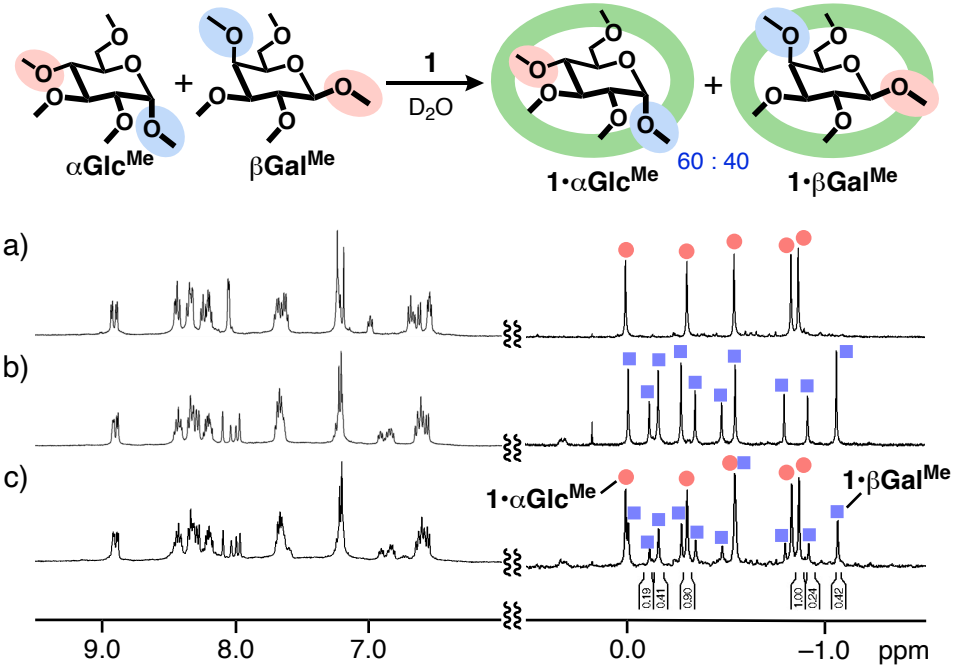

Figure S32. Competitive binding experiment of **1** with **αGlc^{Me}** and **βGal^{Me}** in water. ^{1}H NMR spectra (500 MHz, D_2O, r.t.) of a) **1•αGlc^{Me}**, b) **1•βGal^{Me}**, and c) products after mixing **αGlc^{Me}**, **βGal^{Me}**, and **1**.

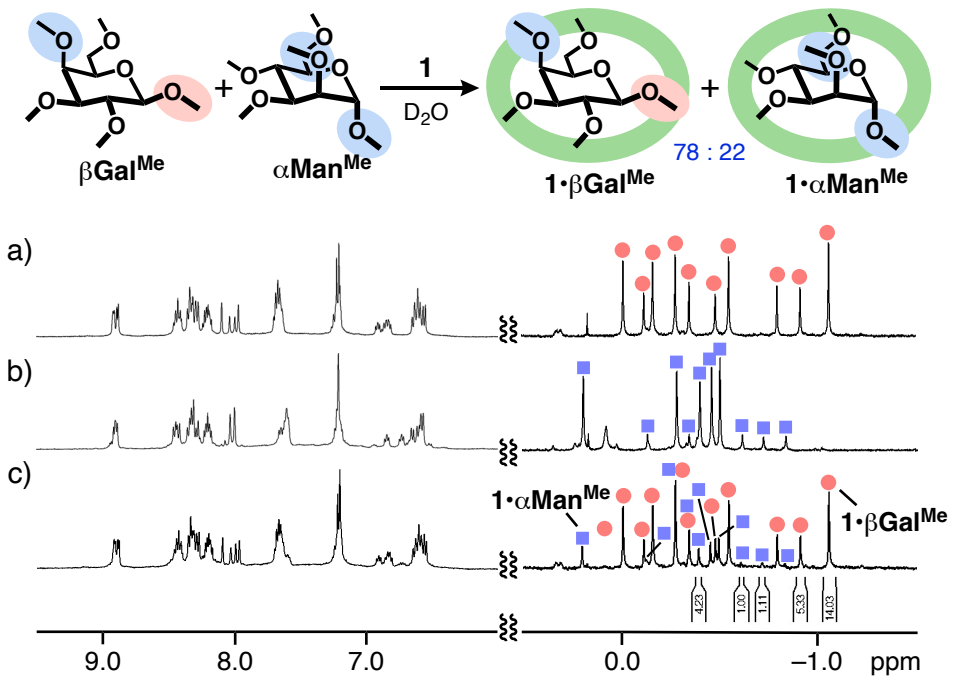

Figure S33. Competitive binding experiment of **1** with **βGal**^{Me} and **αMan**^{Me} in water. ^{1}H NMR spectra (500 MHz, D_2O, r.t.) of a) **1•βGal**^{Me}, b) **1•αMan**^{Me}, and c) products after mixing **βGal**^{Me}, **αMan**^{Me}, and **1**.

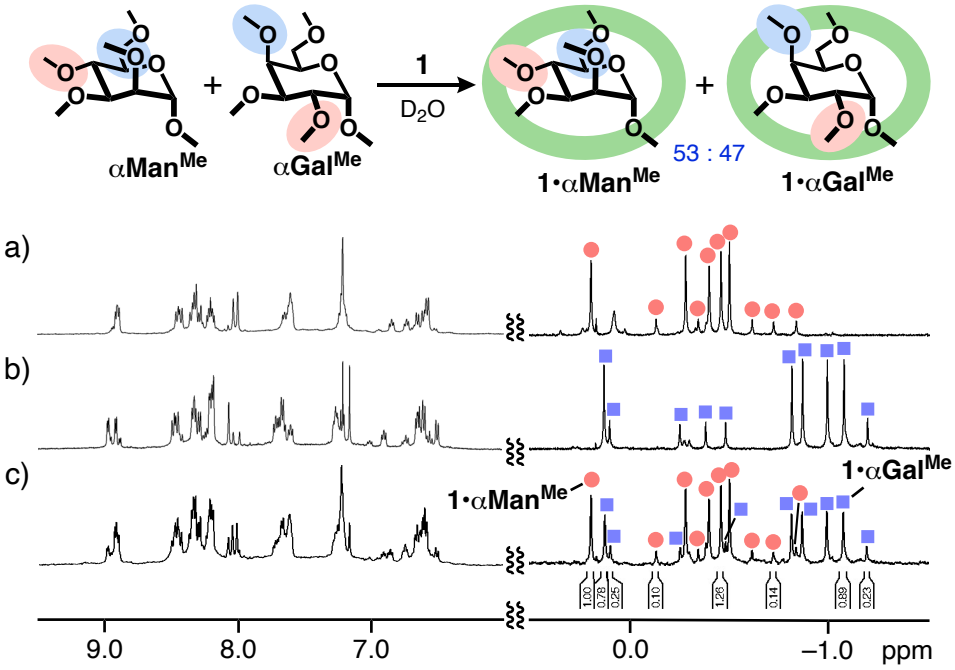

Figure S34. Competitive binding experiment of **1** with **αMan**^{Me} and **αGal**^{Me} in water. ^{1}H NMR spectra (500 MHz, D_2O, r.t.) of a) **1•αMan**^{Me}, b) **1•αGal**^{Me}, and c) products after mixing **αMan**^{Me}, **αGal**^{Me}, and **1**.

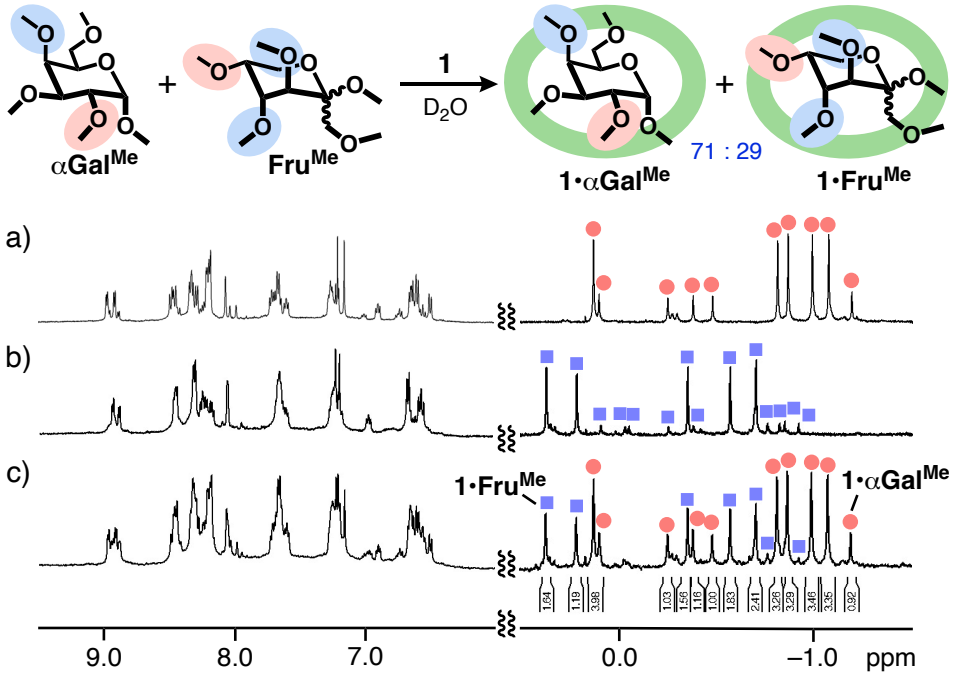

Figure S35. Competitive binding experiment of **1** with **αGal^{Me}** and **Fru^{Me}** in water. ^{1}H NMR spectra (500 MHz, D_2O, r.t.) of a) **1•αGal^{Me}**, b) **1•Fru^{Me}**, and c) products after mixing **αGal^{Me}**, **Fru^{Me}**, and **1**.

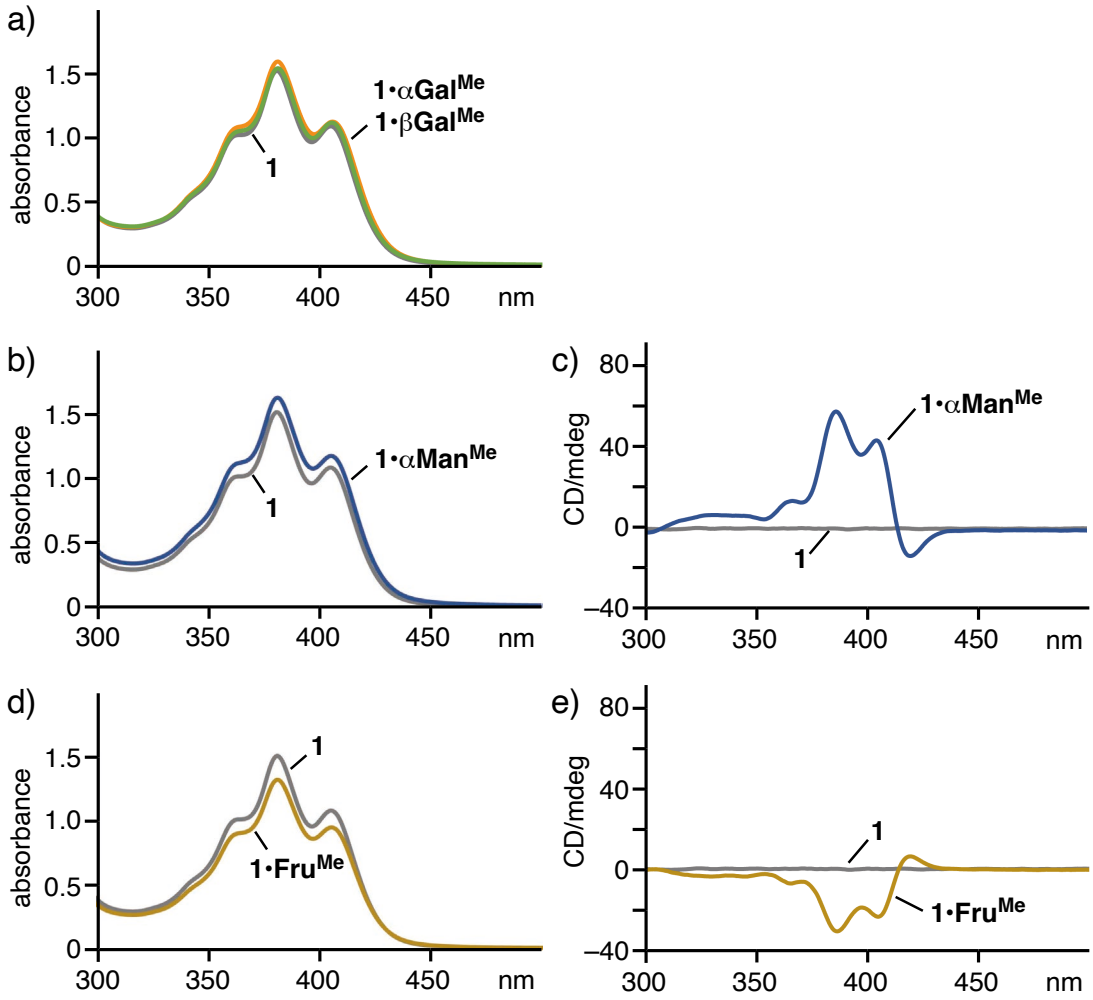

Figure S36. UV-visible spectra (water, r.t., 0.2 mM based on **1**) of a) **1•αGal^{Me}**, **1•βGal^{Me}**, and **1**. b) UV-visible and c) CD spectra (water, r.t., 0.2 mM based on **1**) of **1•αMan^{Me}** and **1**. d) UV-visible and e) CD spectra (water, r.t., 0.2 mM based on **1**) of **1•Fru^{Me}** and **1**.

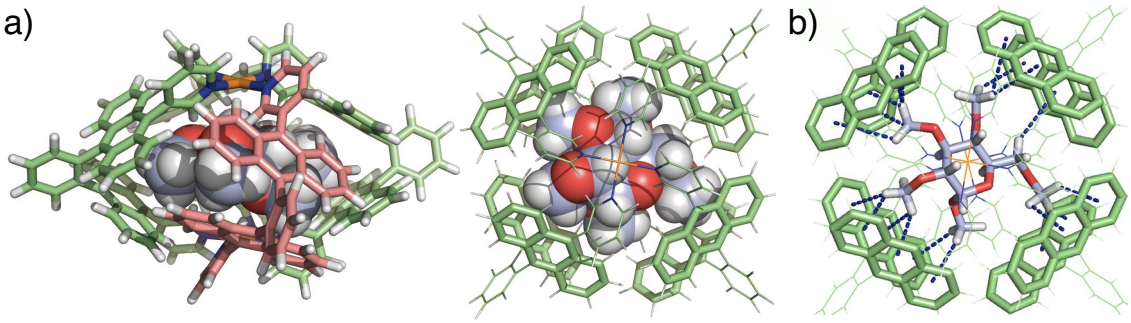

Figure S37. a) Optimized structure of (*P*)-**1•αGlc^{Me}** (side and top views; R = -H for clarity) and b) the highlighted host (anthracene panels)-guest (methyl groups) CH-π interactions in the cavity (dashed blue lines: ≤3.6 Å).

Table S1. Energy changes ($\Delta E_{1\bullet\alpha Glc^{Me}} = E_{1\bullet\alpha Glc^{Me}} - (E_1 + E_{\alpha Glc^{Me}})$ kJ/mol) of capsule **1** (R = H) before and after the encapsulation of **αGlc^{Me}**, calculated by the CAM-B3LYP+D3BJ/LanL2DZ, 3-21G, PCM (H_2O) method.

	E_1	$E_{\alpha Glc^{Me}}$	$E_{1\bullet\alpha Glc^{Me}}$	$\Delta E_{1\bullet\alpha Glc^{Me}}$
(*P*)-**1**	–19486842.5	–2306454.0	–21793771.8	–475.2
(*M*)-**1**			–21793736.8	–440.3

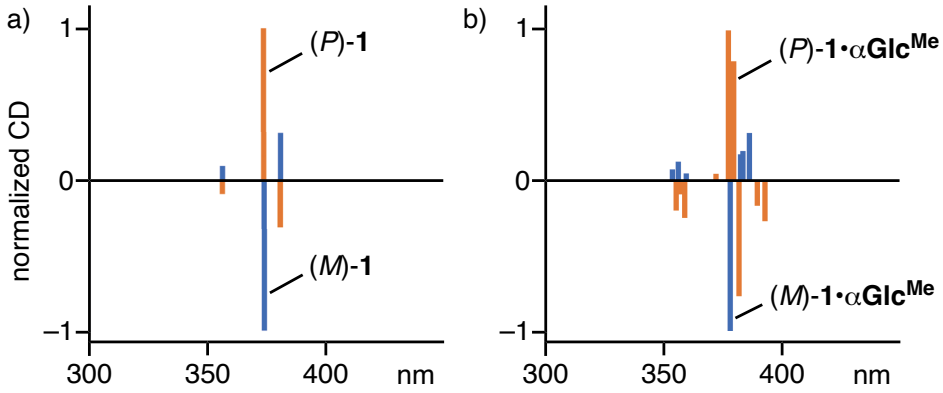

Figure S38. a) Theoretical CD spectra of a) capsules (*P*)/(*M*)-**1** and b) host-guest complexes (*P*)/(*M*)-**1•αGlc^{Me}** calculated by TD-DFT methods (R = H; CAM-B3LYP+D3BJ/LanL2DZ (Pd), 6-31G(d,p) (others), PCM (water) level of theory).

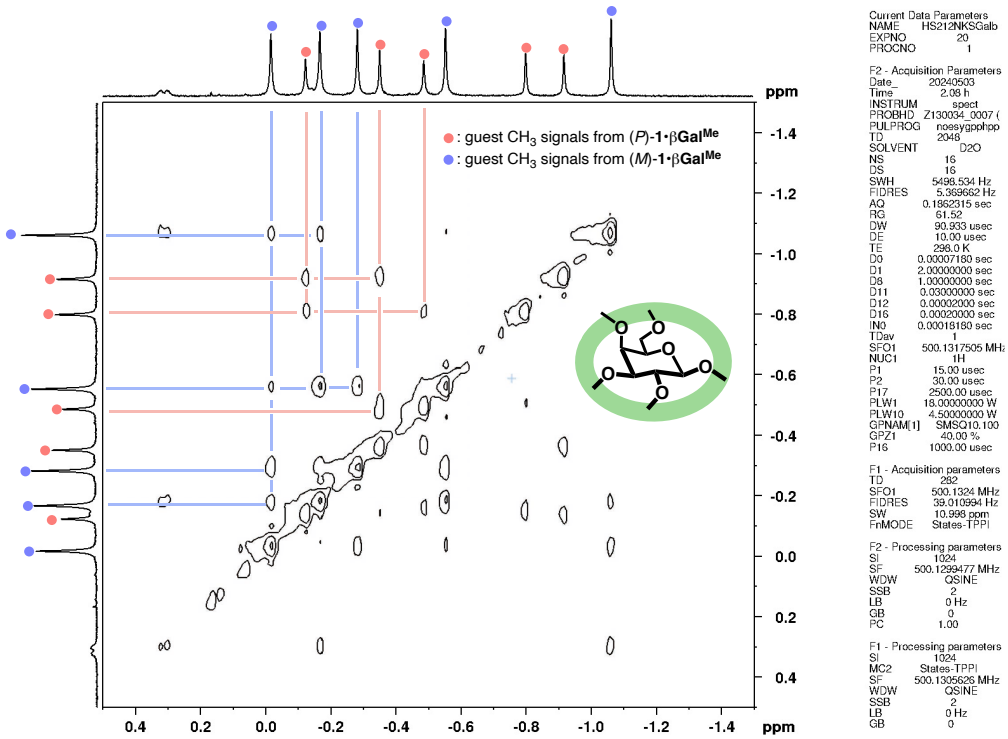

Figure S39a. ^{1}H-^{1}H EXSY NMR spectrum (500 MHz, D_2O, r.t., mixing time = 1.0 s) of **1•βGal^{Me}**.

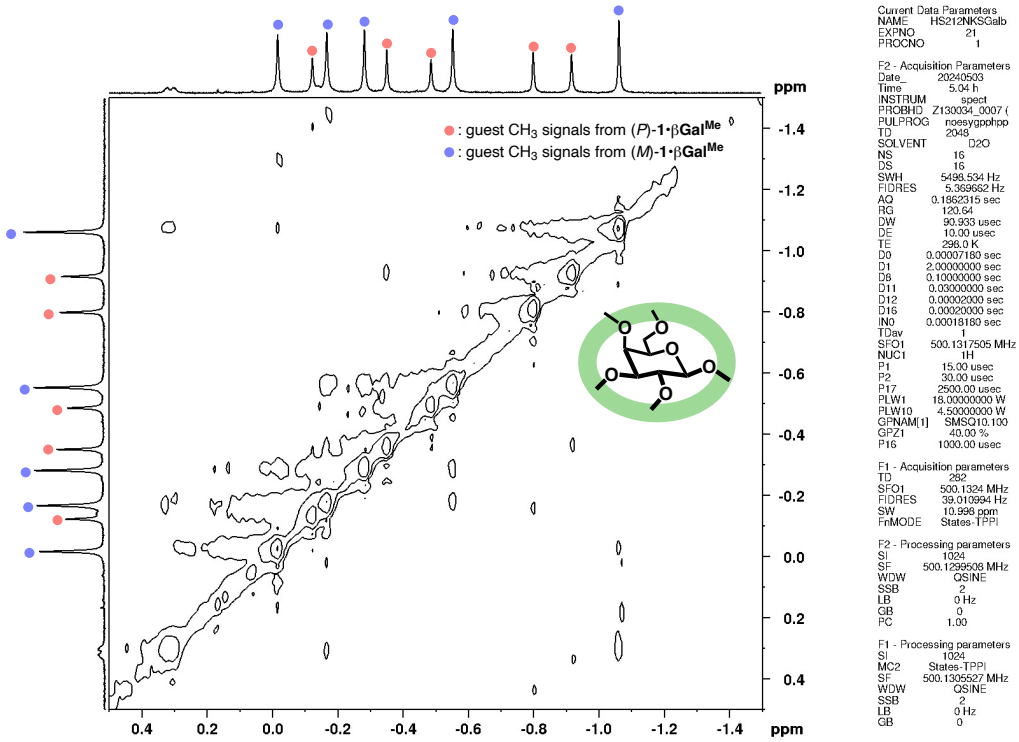

Figure S39b. ^{1}H-^{1}H EXSY NMR spectrum (500 MHz, D_2O, r.t., mixing time = 0.1 s) of **1•βGal^{Me}**.

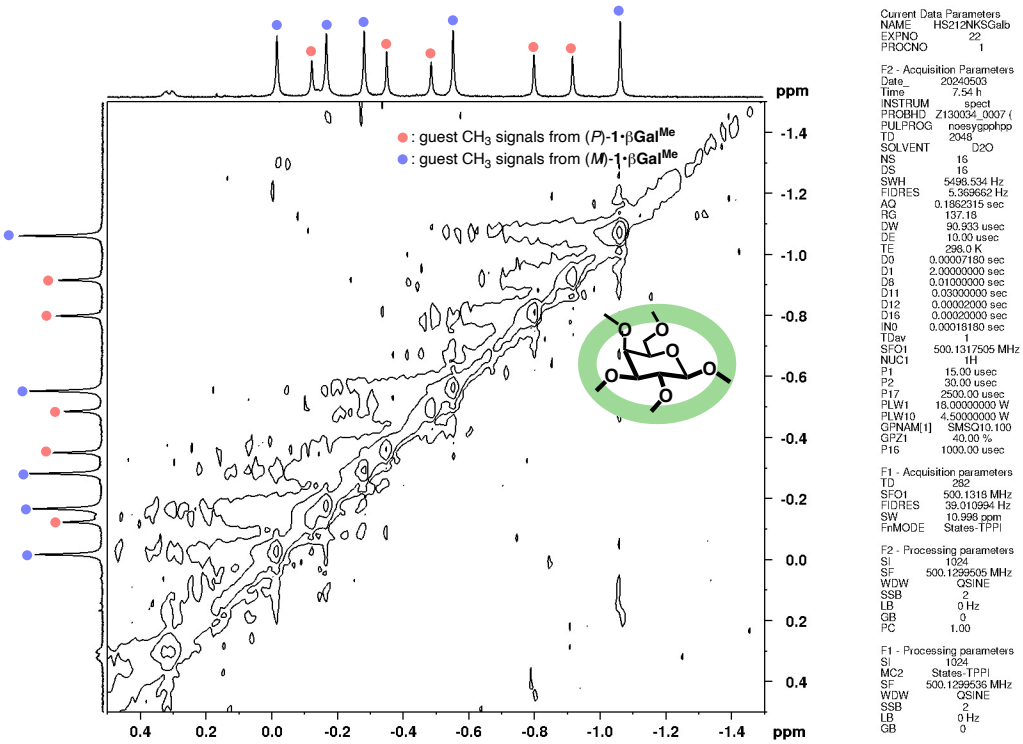

Figure S39c. ^{1}H-^{1}H EXSY NMR spectrum (500 MHz, D_2O, r.t., mixing time = 0.01 s) of **1•βGal^{Me}**.